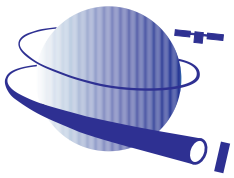

University of Twente
Faculty of Electrical Engineering, Mathematics and Computer Science
Chair for Telecommunication Engineering

Optical phase synchronization in coherent optical beamformers for phased array receive antennas

by

Alejandro García García

Master thesis
Executed from September 2008 to February 2009

Supervisors: dr.ir. C.G.H. Roeloffzen
dr. ir. A. Meijerink
Advisor: ir. Maurizio Burla

Summary

Optical phase synchronization is an important issue in coherent optical beamforming systems. In this kind of architectures, the optical carrier produced by a common laser is split and then modulated by the RF signals coming from different antenna elements, delayed as desired, and combined in couplers. At the combining points it is fundamental that the optical carriers on the two branches are in phase, so that constructive interference can occur at the detector, resulting in maximized optical power and, as a consequence, maximized RF signal power.

The issue of optical phase synchronization becomes particularly sensitive when dealing with hybrid setups, where the integrated optical chips are connected by means of optical fibers. In this case, a number of causes concur to de-synchronize the optical phases, originating destructive interference and dramatically reducing the output signal-to-noise ratio of the system.

In this thesis, several solutions to this problem are proposed and analyzed. The total power feedback loop technique is then chosen as the most suitable approach, and shown to be a valid solution to synchronize the optical phases. Several feedback algorithms are analyzed and simulated in their pros and cons, and then an optimum hybrid algorithm is chosen to allow, at the same time, local maxima avoidance and fast tracking against phase drifts. The performance of this solution was first simulated, optimized in its parameters and finally implemented and tested in the real system.

This work proved that, by means of the designed feedback loop, the optical output power is successfully stabilized at the maximum value despite the drifting in the hybrid setup parameters.

Acknowledgements

A mis padres, Francisco Javier y Carmela, y a mi hermana Irene. Porque todo lo que soy, se lo debo a ellos. Gracias por aguantarme, porque sé que no es nada fácil. Gracias por vuestro apoyo, porque siempre habéis estado ahí para todo lo que he necesitado. Gracias por hacer realidad mis sueños.

I would like to thank my supervisor, dr. ir. C.G.H. Roeloffzen for giving me the opprotunity to do my Master Thesis at the Telecommunication Engineering Group. Also for all the meetings, his useful ideas and the interesting questions. I also want to thank my advisor ir. Maurizio Burla for all his daily support, our long discussions and his advices. Thanks to Arjan and Leimeng, because everytime I have had some questions or doubts, they tried to help me.

Since the first time I arrived at the group everyone have treated me like one of them and have helped me in everything I needed. The less I can do is to thank all of them: the professors Mark Bentum and Wim van Etten; the PhD students: David, Anne, Ricardo, Alex and Rezha; the students: Thomas, Jack, Martin, Liang, Roelof and Pieter; the secretary Lilian and the FC Twente fan: Eduard Bos. I really appreciatte everything you have done for me.

I want to thank all the erasmus students and my football club, VV Drienerlo. They have made my time in the Netherlands so easy and fun. Thank you all, because with you I have lived the best experience of my life.

To conclude but not less important, I would like to thank my very best friends. Because good times or bad times, they are always there for me. I am so lucky for having them with me. Specially I would like to thank my best friend Jaime Lafora, wherever he is.

Resumen

Titulación:	Ingeniería de Telecomunicación
Autor:	Alejandro García García
Tutores:	dr. ir. C.G.H. Roeloffzen
	dr. ir. A. Meijerink
	ir. Maurizio Burla
Institución:	University of Twente
Coordinador Académico:	dr. Arturo Azcorra Saloña
Cotutor UC3M:	dr. Carmen Vázquez García
Fecha de Lectura:	25 de Febrero de 2009
Calificación:	9

INTRODUCCION

Durante los últimos años, la línea de investigación del grupo de Ingeniería de Telecomunicación en la Universidad de Twente (Paises Bajos) ha estado ligada a Radio Frecuencia Fotónica (RFP). Uno de los proyectos que sigue esta línea de investigación es el proyecto SMART (SMart Antenna systems for Radio Transceivers), dentro del proyecto EURIPIDES. El proyecto, formado por un consorcio de numerosas empresas y financiado por el gobierno holandés, comenzó el 1 de Julio de 2005 con el objetivo de desarrollar una antena en la banda K_u para recepción de señales de satélite en aviones usando una antena phased array. El consorcio importante para este proyecto fin de carrera es el consorcio holandés, compuesto por: Universidad de Twente, Lionix BV, NLR y Cyner Substrates.

PHASED ARRAY

En aviónica, las comunicaciones de banda ancha por satélite son necesarias para disponer de internet, previsiones del tiempo o televisión digital. Este proyecto se ha centrado en la recepción de señales digitales por satélite DVB-S. Actualmente la mayoría de las antenas para este propósito son antenas mecánicas, con los inconvenientes que ello acarrea para su uso en aviónica. Por ejemplo la aerodinámica del avión. Por tanto se

ha elegido utilizar una antena de bajo perfil como es una antena phased array. Una antena phased array receptora está compuesta de múltiples elementos y un apropiado procesamiento de señal habilitando la recepción de señales que provienen de una determinada dirección.

En antenas receptoras de fase, la selección del haz que queremos recibir se realiza en la red posterior a la antena. Mediante una red de retardos y combinación de las señales recibidas en los distintos elementos del array, recibimos la dirección deseada. Para cambiar la dirección que deseamos recibir, los retardos deben de ser configurables.

OBFN

El grupo de Ingeniería de Telecomunicación de la Universidad de Twente, es el encargado de desarrollar la red óptica que selecciona el haz en la antena (OBFN). Actualmente se dispone de un 8x1 OBFN con ocho entradas y una salida.

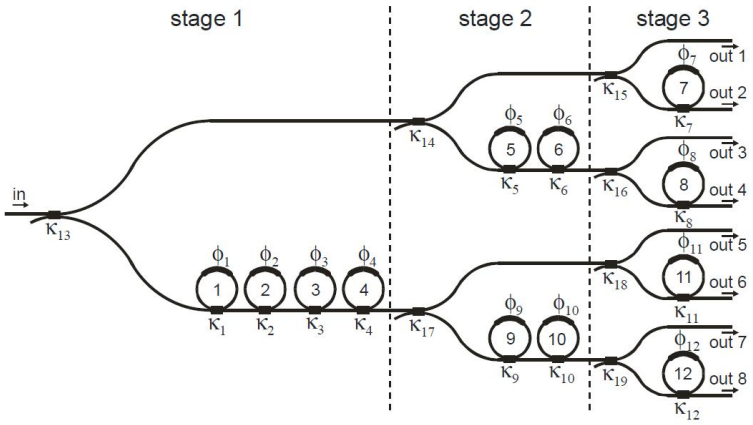

El dominio óptico tiene muchas ventajas con respecto al dominio eléctrico:

- Pequeño tamaño.
- Bajo coste.
- Independencia de frecuencia.
- Inmunidad ante interferencias electromagnéticas.
- Gran ancho de banda.

Los elementos ópticos que proveen los retardos son anillos resonadores ópticos. El problema de este elemento es que al aumentar el ancho de banda el retardo disminuye y viceversa. Para solucionar este problema, en lugar de utilizar un único anillo resonador óptico, se utilizan varios en cascada.

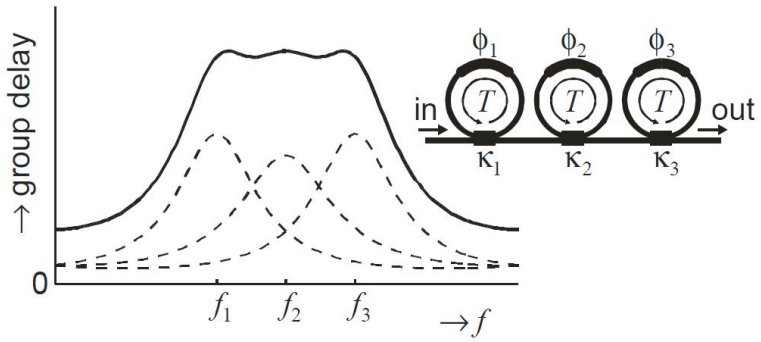

SISTEMA ANTENA RECEPTORA

El sistema utilizado está compuesto por una antena receptora phased array. Después se realiza una conversión del dominio eléctrico al óptico. Una vez en el dominio óptico se utiliza el OBFN, que es configurado por medio de un sistema de control. A la salida del OBFN se realiza la conversión al domino eléctrico de nuevo para recibir la señal de televisión.

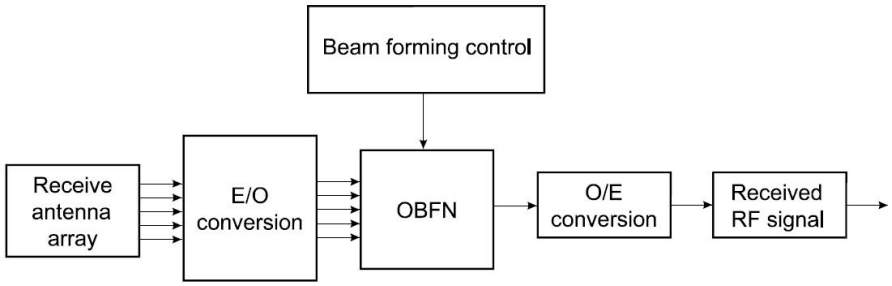

Para realizar la conversión al dominio óptico se utiliza un solo láser como señal portadora. Esta señal se divide en el número de antenas de que dispone el phased array. Cada señal portadora óptica es modulada por la señal que recibe cada elemento del array. La señal modulada es la que entra al OBFN. A su vez para realizar la conversión al dominio eléctrico tras el OBFN se utiliza un fotodiodo.

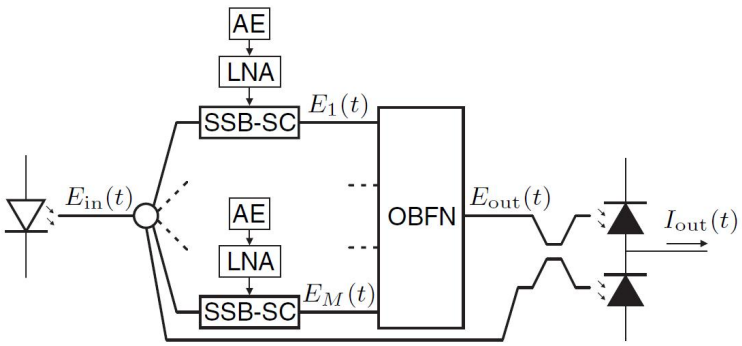

El control del OBFN se realiza por medio de un sistema externo. Este sistema de control aplica calor en la guía por medio de tensión para modificar los parámetros

de los ORR, los combinadores y los desfasadores. Para ello se dispone de un interfaz gráfico implementado en JAVA que se comunica con el sistema de control.

PROBLEMA DE SINCRONIZACION DE LA FASE OPTICA

El problema que aparece en este sistema se debe al uso de un solo láser como portadora óptica. En el interior del OBFN se combinan las diferentes señales procedentes de los elementos de la antena de dos en dos. Por tanto, en los puntos donde se combinan las señales, la sincronización de la portadora óptica es un requisito. Si se produce una desincronización, a la salida del OBFN la potencia de la señal recibida no será máxima.

El OBFN actualmente es un chip en el que no todo el sistema está integrado. Las interconexiones se realizan por medio de fibras ópticas externas, por lo que el sistema es muy sensible a variaciones de temperatura y cualquier ligero movimiento. Cualquier variación de este tipo hace que la potencia de la señal a la salida del OBFN disminuya. Para intentar solucionar estos problemas se ha instalado el sistema dentro de una caja de espuma de poliestireno, pero aún así no es suficiente. Por este motivo es necesario sincronizar la fase óptica en el interior del OBFN.

La solución es utilizar desfasadores. Se coloca un desfasador antes del punto donde se combinan las señales, en la rama superior. En total, en un OBFN de N entradas, el número de desfasadores es N-1. De esta forma, aplicando un desfase a una de las señales se logra la sincronización de ambas portadoras ópticas.

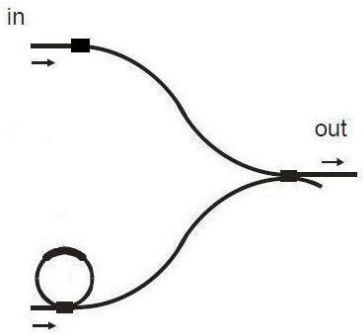

LAZO REALIMENTADO

El método utilizado para sincronizar la fase óptica es mediante un lazo realimentado. Un circuito externo mide la potencia a la salida del OBFN, y en función de su valor, configura los desfasadores de forma que obtengamos la máxima potencia de señal.

El lazo realimentado está ejecutando continuamente los siguientes pasos:

1. **Medir la potencia de la señal RF:** Primero se mide la potencia de la señal RF. Para medir la potencia se hace uso de un analizador de espectros a la salida del sistema, después del fotodiodo. Por medio de un PC y del programa LabVIEW,

interactuamos con el analizador de espectros para obtener la potencia de señal. Este paso es muy importante porque el nuevo valor del desfasador se calcula en base a éste parámetro.

2. **Algoritmo:** El algoritmo calcula los nuevos valores de los desfasadores de forma que alcancemos la máxima potencia a la salida en el menor número de pasos. Se implementa en LabVIEW gracias a un script de Matlab.

3. **Configurar los desfasadores:** Finalmente el lazo tiene que cambiar el valor de los desfasadores. Para configurar los desfasadores simplemente se interactúa con el sistema de control. Se envía el comando correcto al sistema de control, y es éste el que se encarga de configurar adecuadamente el valor que le hemos mandado. Para comunicarnos con el sistema de control, el PC se conecta mediante un cable USB a este sistema, y gracias a LabVIEW podemos interactuar con él.

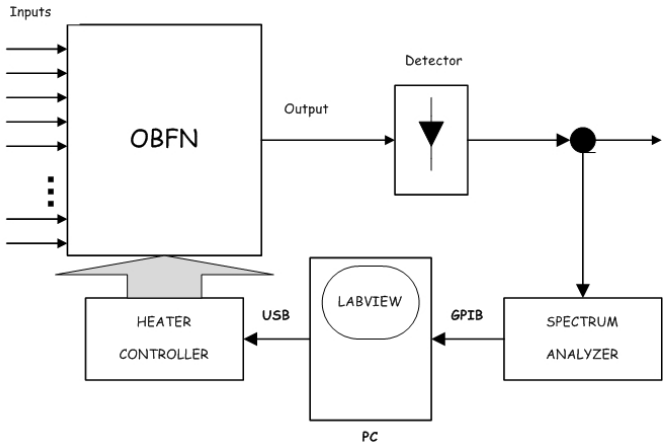

ALGORITMO DEL LAZO REALIMENTADO

La parte más importante del lazo realimentado es el algortimo. Debido a su fácil implementación, el estudio comienza con un algoritmo de búsqueda local: el algoritmo Hill Climbing. El algoritmo se ejecuta cíclicamente: primero configura un desfasador un numero de iteraciones y al terminar, comienza con otro desfasador. Cuando termina el último desfasador comienza de nuevo por el primero.

Los parámetros del algoritmo son los siguientes:

- *Umbral de potencia:* La potencia a la salida debe ser mayor que éste umbral.
- *Paso Grande:* Parámetro para mover el desfasador rápido.
- *Paso pequeño:* Parámetro para mover el desfasador lento. Este es el paso por defecto.

- *Dirección del desfasador:* El razonamiento para cambiar el desfasador se asemeja a una barra, por lo que la dirección para mover la barra puede ser izquierda o derecha. Utilizamos como inicialización que el desfasador aumenta: dirección derecha.

El funcionamiento del algoritmo es el siguiente:

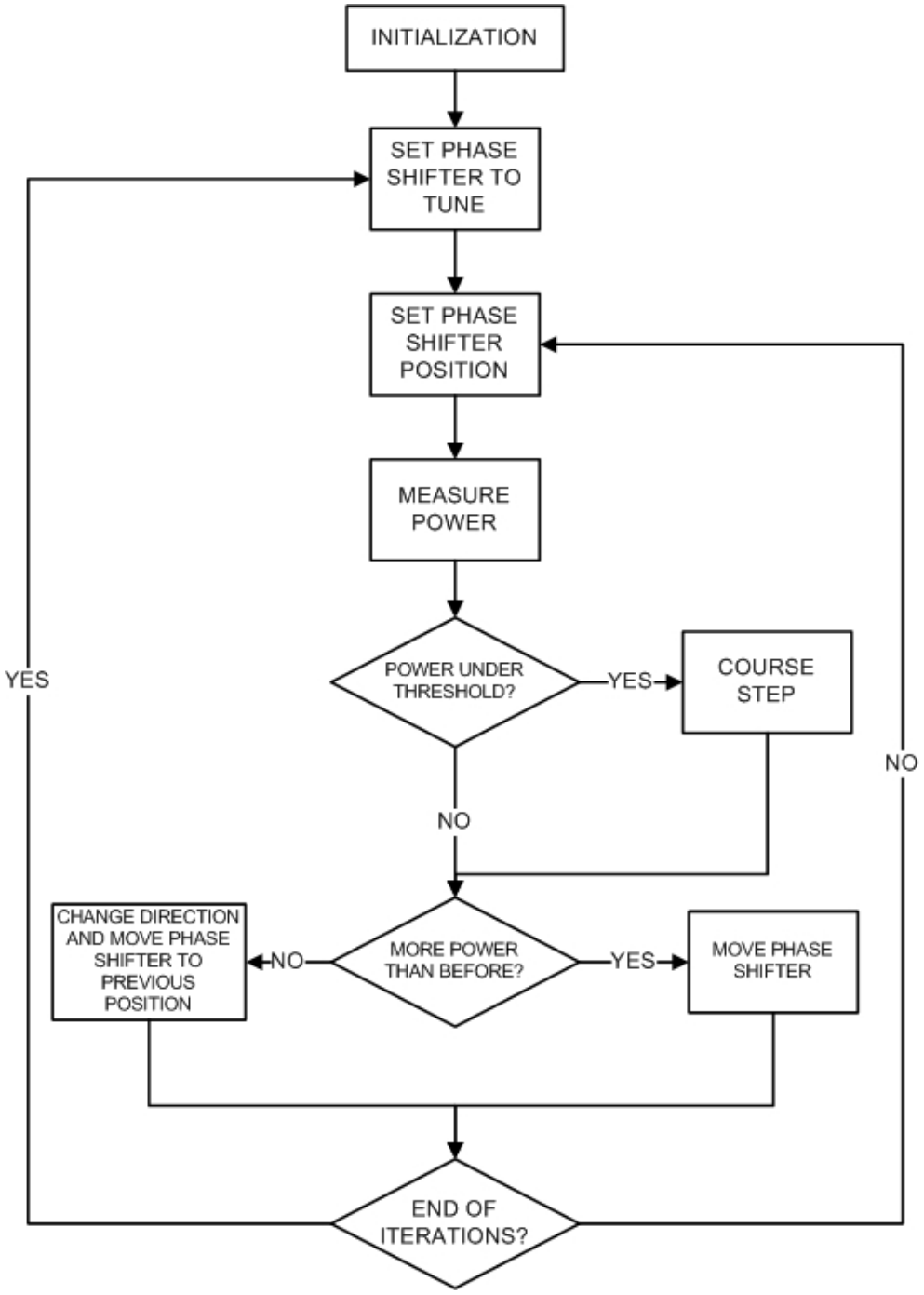

Este tipo de algoritmos ofrecen seguimiento cuando la potencia comienza a disminuir, pero el problema que tienen es que al encontrar un máximo local, una meseta

o un risco, se quedan estancados en ese valor y no llegan a obtener el máximo global, que es lo que deseamos. Por este motivo este tipo de algoritmos no son válidos.

Por tanto el estudio prosigue con un algoritmo de búsqueda global: algoritmo genético. Este tipo de algoritmos generan una población de posibles soluciones, llamados individuos, que evolucionan hacia una mejor solución. Su funcionamiento es el siguiente:

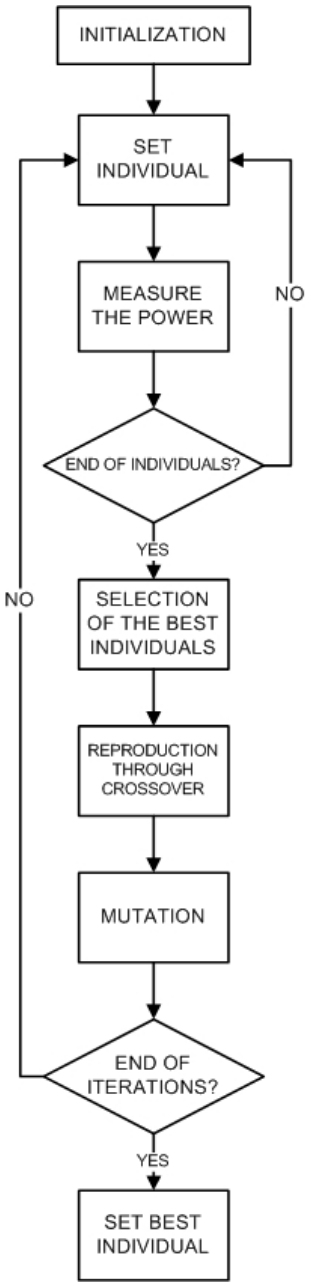

La represenatción de los individuos se realiza en binario. Cada desfasador varía desde 0 a 3000 en decimal, por lo que para representar cada desfasador en binario se necesitan 12 bits. Por tanto cada individuo será la concatenación de todos los desfasadores en binario.

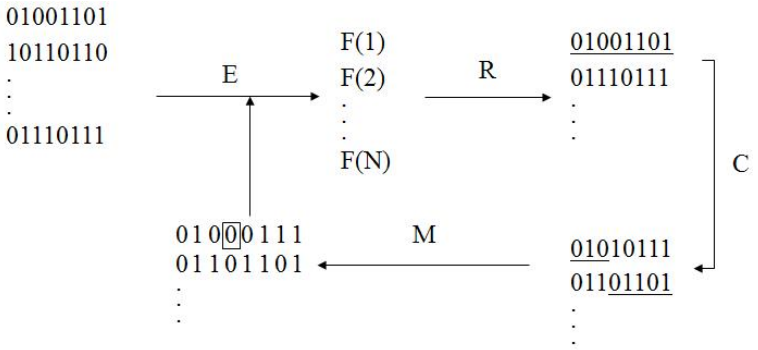

Mediante este algoritmo nos aseguramos que hemos alcanzado el máximo global, pero en cambio no ofrece seguimiento. Una vez que ha finalizado de ejecutar, si la potencia a la salida disminuye debido a la desincronización de la fase óptica, tenemos que ejecutar el algoritmo desde el principio, y esto es ineficiente.

La solución es combinar ambos algoritmos:

1. **Algoritmo Genético:** Primero se ejecuta el algoritmo genético. Al finalizar hemos obtenido el máximo global de la potencia a la salida del OBFN.

2. **Algoritmo Hill Climbing:** Una vez el algoritmo genético ha finalizado, comienza el algoritmo hill climbing. Los valores de los desfasadores calculados por el algoritmo genético se usan como inicialización del algoritmo hill climbing. Éste algoritmo ofrece seguimiento, por lo que si la potencia a la salida disminuye, el algoritmo mantendrá la potencia en el máximo global simplemente cambiando la posición de los desfasadores uno por uno, cíclicamente.

MEDIDAS EN EL LABORATORIO

Una vez concluido el estudio del lazo realimentado para sincronizar la fase óptica, pasamos al laboratorio para probar su correcto funcionamiento. Las medidas se realizaron sobre un chip 8x1 OBFN, utilizando simplemente dos entradas y 1 salida, por lo que sólamente se necesita utilizar un desfasador. La señal simulada es una onda fontal, por lo que no hace falta utilizar ningún ORR para retardar las señales.

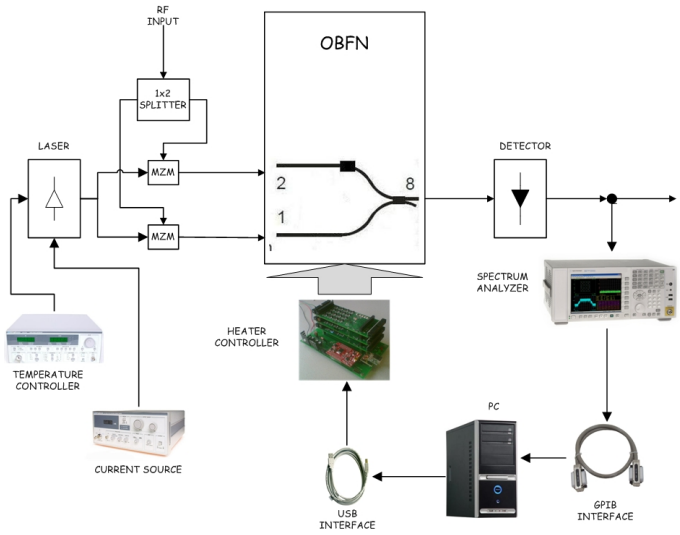

Primero se utilizó como señal de entrada una señal conocida: un tono RF generado por un analizador de espectros en la frecuencia del transpondedor central de la señal DVB. Comenzamos configurando los parámetros del algoritmo hill climbing. Una vez conseguido, se probó el algoritmo implementado para el lazo realimentado (Algoritmo genético + Algoritmo hill climbing), comprobando que efectivamente se logra sincronizar la fase óptica logrando mantener la potencia a la salida en su máximo valor.

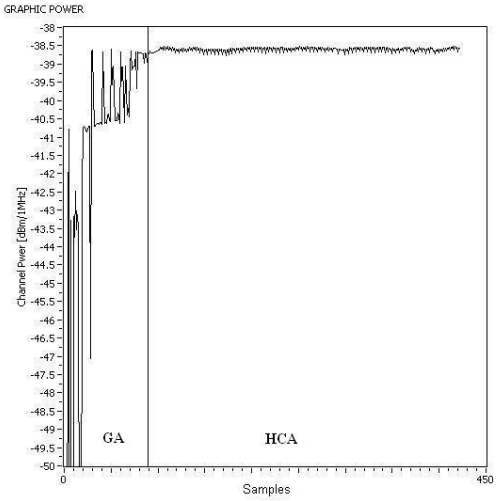

El último test se realizó utilizando la señal para la que el sistema se va a utilizar: una señal DVB. La señal se recibe mediante una antena parabólica alineada con el satelite Astra 19.2E. Tras ejecutar el lazo realimentado, se puede comprobar como la potencia de dicha señal a la salida del sistema se mantiene en su máximo valor. Se pueden apreciar claramente los transpondedores de la señal DVB en el analizador de espectros tras el paso por el OBFN.

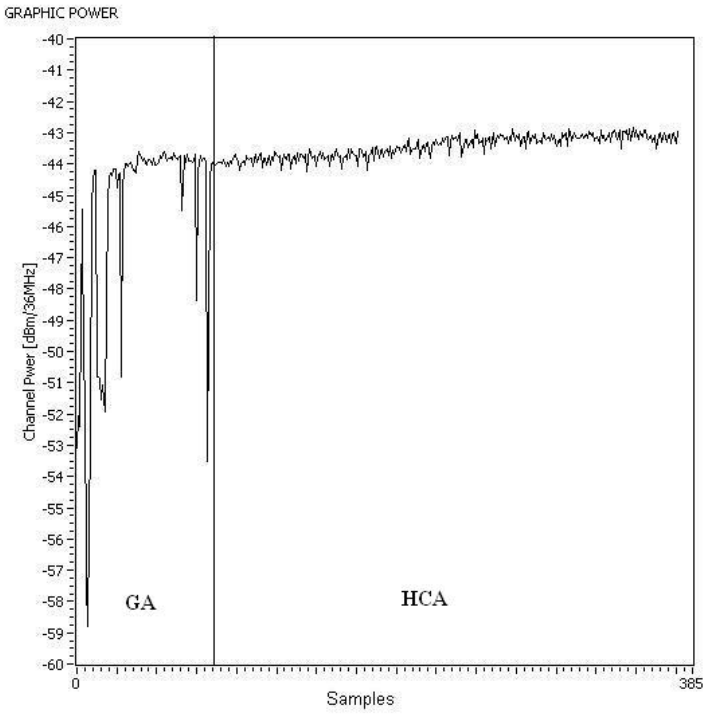

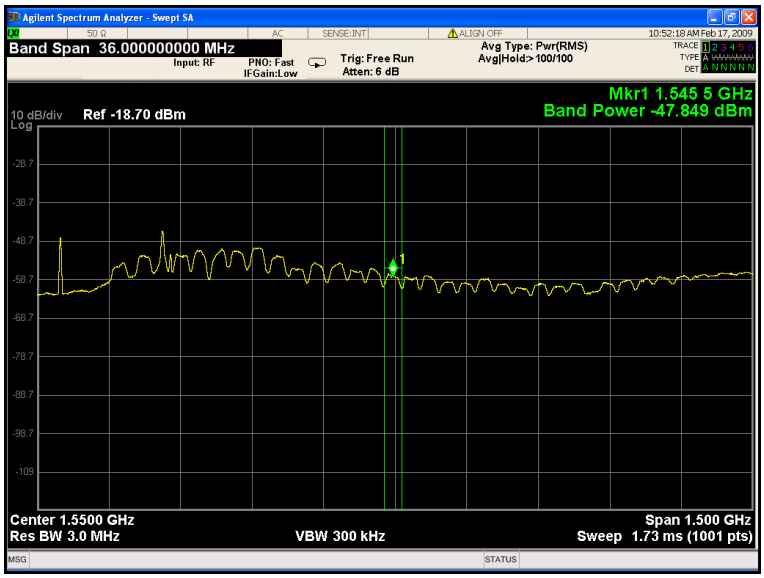

Por tanto, podemos concluir que utilizar un lazo realimentado basado en la potencia a la salida del OBFN soluciona el problema de la sincronización de la fase óptica.

RECOMENDACIONES

El primer paso para sincronizar la fase óptica ha sido conseguido, pero la investigación debe continuar.

- Primeramente el algoritmo se tiene que probar en diferentes escenarios. El primer escenario sería simular la recepeción de una señal desde una dirección distinta a la frontal (como hasta ahora). Después de esto lo ideal sería extender el sistema de un OBFN 2x1 a uno 4x1, 8x1 y así sucesivamente.

- La investigación del algoritmo es muy importante. Otros algoritmos pueden ser estudiados. Además se pueden realizar mejoras en el algoritmo ya implementado. Por ejemplo, que el algoritmo genético no tenga que esperar a que realice todas las iteraciones sino que si primero alcanza una determinada potencia de señal, se pare.

- El paso final para un futuro trabajo sería diseñar una placa PCB que implemente el lazo realimentado.

Contents

List of Figures

List of Symbols and Abbreviations

Symbols

$r(t)$	amplitude of signal from antenna element
$s_m(t)$	m^{th} RF input signal from antenna element
T_m	delay value of m^{th} antenna element
α_m	amplitude weighting factor of m^{th} input signal from antenna element
$\psi_s(t)$	phase of input signal from antenna element
$v_m(t)$	down converted input signal from antenna element

Abbreviations

AE	Antenna Element
BBP	Broadband Photonic
BPB	Broadband Photonic Beamformer
BFN	Beam-forming Network
CATV	Community Antenna Television
CIMNE	International Center for Numerical Methods in Engineering
CFG	Chirped Fiber Grating
CNAM	Conservatoire National des Arts et Metiers
DAC	Digital to Analog Converter
DFB	Distributed FeedBack
DSB	Double-Side Band

DSB-SC	Double-Side Band Suppressed Carrier
DVB	Digital Video Broadcasting
DVB-DSNG	DVB-Digital Satellite News Gathering
DVB-S2	DVB-Satellite version 2
EADS	European Aeronautic Defence and Space Company
EMI	ElectroMagnetic Interference
EURIPIDES	Eureka Iniciative for Packaging & Integration of microDevices and Smart Systems
FRAM	Ferroelectric Random Access Memory
FSR	Free Spectral Range
GA	Genetic Algorithm
GPIB	General-Purpose Instrumentation Bus
GUI	Graphical User Interface
HCA	Hill Climbing Algorithm
IF	Intermediate Frequency
IMD-2	Second order InterModulation Distortion
LabVIEW	Laboratory Virtual Instrumentation Engineering Workbench
LAN	Local Area Networks
LNA	Low-Noise Amplifier
LNB	Low-Noise Block
LCD	Liquid Crystal Display
LED	Light Emitting Diode
LIA	Lock-In Amplifier
LO	Local Oscilator
MZI	Mach-Zender Interferometer
MZM	Mach-Zender Modulator

MEMPHIS	Merging Electronics and Micro & nano-PHotonics in Integrated Systems
MVC	Model View Control
NLR	National Aerospace Laboratory (Netherlands)
OBFN	Optical Beam Forming Network
OCDMA	Optical Code Division Multiple Access
OSBF	Optical SideBand Filter
ORR	Optical Ring Resonator
PAA	Phased Array Antenna
PCI	Peripheral Component Interconnect
PAN	Personal Area Networks
PCB	Printed Circuit Board
PID	Proportional-Integral-Derivative
PSTN	Public Switched Telephone Networks
RIN	Relative Intensity Noise
RFP	Radio Frequency Photonics
RoF	Radio-over-Fiber
SATCOM	SATellite-based COMmunication
SMART	SMart Antenna systems for Radio Transceivers
SPI	Serial Peripheral Interface
SSB	Single-Side Band
SSB-SC	Single-Side Band Suppressed Carrier
TTD	True Time Delay
UART	Universal Asynchronous Receiver and Transmitter
UT-TE	Telecommunication Engineering group of the University of Twente
VISA	Virtual Instrument Software Architecture

Chapter 1

Introduction

This chapter describes the background that can be regarded to understand the framework in which the master thesis is developed. At the end of this chapter, the assignment goal and the thesis organization are given.

1.1 Background

In past years Radio Frequency Photonics (RFP) has been one of the major research fields at the Telecommunication Engineering group of the University of Twente (UTTE) [1]. The applications of this research field are in the Public Switched Telephone Networks (PSTN), Local Area Networks (LAN) and Personal Area Networks (PAN), distribution of Community Antenna Television (CATV) signals, and Phased Array Radar Systems. One of the most important fields of research is optical processing and beamforming networks. The current projects are:

- Phased-Array Communication antennas for Mass-market Application Needs (PACMAN)
- Dynamically Reconfigurable Broadband Photonic (BBP) Access Networks
- SMart Antenna systems for Radio Transceivers (SMART)
- Broadband Photonic Beamformer (BPB)
- Merging Electronics and Micro & nano-PHotonics in Integrated Systems (MEMPHIS)

The last three projects enumerated above are in the field of optical beamforming. For this reason, the issue of optical phase synchronization is important in all of them. The same concept to synchronize the optical phase is used, but the final implementation will be different for each application.

1.1.1 The SMART project

In this master thesis, we will focus on an implementation of the OBFN for the SMART project. The SMART project [2] is part of the Eureka Iniciative for Packaging & Integration of microDevices and Smart Systems (EURIPIDES) [3] and is supported by the Dutch Ministry of Economic Affairs. From 1st July 2005 the SMART project has been developing to achieve global leadership of Europe in wireless markets and applications. Consortium companies are: International Center for Numerical Methods in Engineering (CIMNE), Conservatoire National des Arts et Metiers (CNAM), Cyner Substrates, European Aeronautic Defence and Space Company (EADS), LioniX BV [4], National Aerospace Laboratory (Netherlands) (NLR), RADIALL, Sistemas Radiantes F. Moyano and UT-TE. The products developed for this consortium will have to be able to offer a high efficiency based on the adequate interconnection and packaging technologies for the project's antenna. These may be used either to achieve a higher coverage for the global networks and/or to reduce the transmission power to save batteries and to reduce health impact for the user. EMC compatibility issues within a multi-standard environment is of great concern.

The consortium that is relevant to the system described in this master thesis is the one based in the NL, consisting of UT-TE, LioniX BV, NLR and Cyner Substrates. This consortium is developing technology for such conformal airborne antennas. This technology development includes two key topics: a broadband conformal K_u-band antenna and a broadband OBFN. UT-TE is focused in the implementation of the broadband OBFN, in cooperation with LioniX.

1.2 Phased Array Antenna and Beam-forming Network

SATCOM For enhanced airbone communication, antenna systems with broadband SATellite-based COMmunication (SATCOM) capabilities are required. Nowadays, satellite tracking is achieved most of the time by mechanically steering a reflector antenna in the transmitting or receiving directions as in Figure 1.1. In some applications, for instance on an airplane, this can be very inconvenient because of air drag and mechanical reliability. The installation of such systems onboard of an aircraft would be much easier using a very low profile antenna, able to point to satellites anywhere in the upper hemisphere. For this purpose, Phased Array Antennas (PAAs) conformal to the aircraft fuselage as in Figure 1.2, are attractive options [5].

Phased Array Antenna A PAA consists of multiple Antenna Elements (AEs) and an appropriate signal processing network, enabling direction-sensitive transmission and/or reception of electromagnetic waves. Thus by controlling the progressive phase difference between the elements, the direction of maximum radiation can be steered in any desired

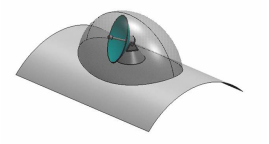

Figure 1.1: Mechanically steered reflector antenna

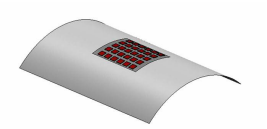

Figure 1.2: Conformal phased array antenna

position. Since in many applications like airbone satellite tracking, it is desirable to have a continuously variable scanning direction, the system should be capable of continuously varying the phase relation between the elements [6]. As mentioned before, PAA have several advantages:

- System size and weight can be reduced by using phased array antennas. This is critical for satellite and airplane applications.
- Beam-shaping capabilities offered by PAAs allow a more efficient use of transmission energy. This is beneficial for the battery lifetime of mobile devices and also to have less interferences and health hazard.
- With PAA it is possible to realize multi-beam systems. This produces an increase in capacity, both bit/s or bandwidth (spectrum efficiency) and users per sector, using the space-division multiplexing technique. Figure 1.3.

Beam-forming Network In receiving mode each individual AE signal consists of a time-delayed version of some desired signals plus possible time-delayed versions of undesired signals (from different directions). The values of these time delays vary for each AE, and depend on the geometrical distribution of the AEs and the direction of the incoming wave front. The signal processing part therefore consists of a delay-and-combine network that equalizes the delay values of the signal terms that correspond to the desired received signal, such that the desired signal terms add up in phase and are reinforced, whereas the undesired signal terms add up in uncorrelated phase and are hence suppressed. The time delays should be tunable to be able to alter the viewing angle of the PAA. When only the time delays are tunable such processing is called beam steering. When the amplitudes of the AE signals are also controlled we talk about Beam-forming Network (BFN). The signal processing circuit is then called a beam forming network [7]. It is shown in Figure 1.3.

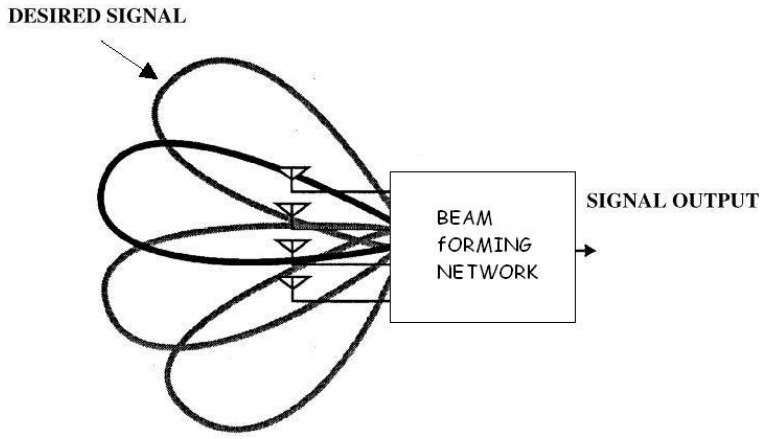

Figure 1.3: Phased array antenna receiver system

1.2.1 Optical Beam Forming Network (OBFN)

Conventional phased array antennas using waveguide or coax for signal distribution are impractical for large scale implementation on satellites or spacecraft. They exhibit prohibitively large system size, heavy weight, high attenuation loss, limited bandwidth, sensitivity to ElectroMagnetic Interference (EMI) temperature drifts and phase instability. For these reasons the optical domain is used. Implementing the BFN in the optical domain shares many common advantages with other RFP signal processing techniques such as:

- Compactness and light weight.
- Low loss.
- Frequency independence.
- Large instantaneous bandwidth.
- Inherent immunity to EMI.

However, OBFN also has some disadvantages like, for instance, the need of conversion from electrical to optical, and from optical to electrical.

1.2.2 Ring Resonator-Based Optical Beam Forming Networks

Most previously proposed optical beamformer systems are either based on optical phase shifters or switchable delay matrices. However, phase shifters do not provide True Time Delay (TTD), and therefore result in a frequency-dependent beam angle and shape (beam squint). Switchable delay lines, in turn, do not provide continuosly tunable beam direction.

These limitations can be overcome by the use of a continuosly tunable TTD element. A typical structure of an Optical Ring Resonator (ORR) delay line is illustrated in Figure 1.4. At the beginning a portion of the light coming from the straight waveguide is coupled into the ring-shaped waveguide, and then after each roundtrip, a portion of the light in the ring is coupled out at the proportion as good as that of the coupling-in process. Meanwhile, the rest of the light stays in the ring and goes on for the next roundtrip, which realizes the structural enhacement. ORRs are using planar waveguide technology, which, in fabrication, can be highly integrated in small chips. Thermal tuning mechanism can be used in ORRs, which facilitates an accurate tuning of the delay [8].

Injecting a light pulse in the input, the ORRs give an infinite number of discrete pulses at the output. Each pulse is proportionally lower than the previous one and is delayed from the previous one by one roundtrip time $T = \frac{L}{v}$, with L being the physical length of the optical ring resonator, and v the velocity at which the signals travel in it. $\frac{1}{T}$ is the Free Spectral Range (FSR) of the ORR. An ideal lossless ORR section acts as an optical all-pass filter, which is characterized by a unity magnitude response. It has a periodic group delay, which represents the effective time delay to the RF signal that is modulated on the optical carrier signal. Within one FSR of the group delay response a delay peak is centered at the resonance frequency, which is intended to be used to delay the RF signal. The peak value of the delay and the resonance frequency are determined by the tunable parameters k and ϕ, respectively, which facilitates the continuous tunability of the ORR-based delay element. However, the peak value of the delay is more or less inversely proportional to the peak width. Hence, when the peak delay value of the ORR is increased, the bandwidth decreases, revealing an inherent tradeoff of the ORR-based delay. It is shown in Figure 1.4.

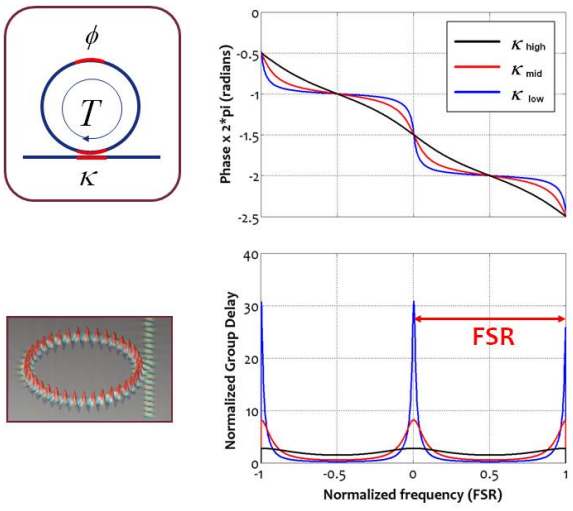

Figure 1.4: Optical Ring Resonator

For a broadband RF signal a single ORR may not provide enough delay bandwidth. In this case multi-ring delay elements can be used instead. A multi-ring delay element is built by cascading multiple ORR sections, as shown in the inset of Figure 1.5. Each ring can be tuned independently, and the individual group delay responses superpose to form the eventual group delay response of the multi-ring delay element. When the rings are properly tuned, to different resonance frequencies, a group delay response with a flattened delay band can be achieved. It can be seen that delay ripples appear in the flattened delay band, but can be reduced to an acceptable level by squeezing the resonance frequencies closer to each other or by adding more rings in the cascade. Hence, multi-ring delay elements show an inherent trade-off between peak delay, bandwidth, delay ripple and number of rings [7].

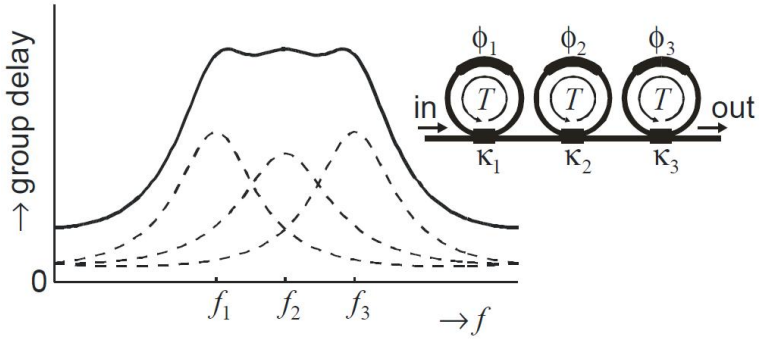

Figure 1.5: Theoretical group delay response of three cascaded ORR sections

1.3 Assigntment goal

This Thesis has been developed on the basis of a Master assignment. The goal is to design and test the scheme that synchronizes the optical phases of the signals that are combined in the OBFN, so that the power of the output signal of the optical beam former is maximized, even when part of the beam former setup is based on fibers.

1.4 Thesis organization

There are in total seven chapters in this Thesis. After the assigntment background and motivations given in this Chapter, the receiver architecture used is explained in Chapter 2. The description of the optical phase syncronization problem and the different solutions are introduced in Chapter 3. In Chapter 4, the design of the feedback loop is discussed. Then the implementation of the algorithm is explained in Chapter 5. In Chapter 6 the measurement results are shown. Finally in Chapter 7, the conclusions and recommendations for future work are given.

Chapter 2

Optical Beam Forming System

The architecture for an optical beam forming system is represented in Figure 2.1:

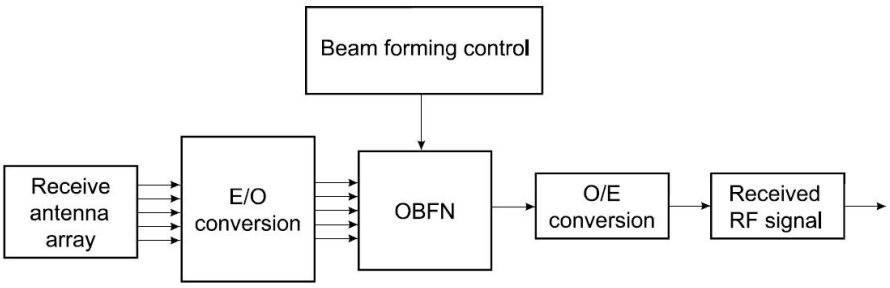

Figure 2.1: System design of a receive antenna with OBFN

As we can see, the phased array antenna receives the RF signal from any spatial point, and after this, the signal is down-converted. Then, an electrical to optical conversion is needed afterwards in order to be able to use our OBFN. Finally, an optical to electrical conversion is also needed. All the processing steps described will be further explained in the upcoming paragraphs.

2.1 Received RF wave

As we said in the previous chapter, this master thesis is in the framework of the SMART project, where the application is satellite communications. The received satellite signal consists of a horizontally and a vertically polarized wave, both spanning a frequency range of 10.7-12.75 GHz, in the K_u-band. This range is divided in frequency slots with center frequencies $f_{RF,n}$, typical transmission bandwidths of 26 to 36 MHz, and guard bands between the slots of at least 4 MHz, as illustrated in Figure 2.2. These slots correspond to the separate transponders in the satellite. The center frequency sets $f_{RF,n}$ are chosen differently for the two polarizations, in such a way that the center frequencies in one polarization fall in the guard bands of the other polarization, in order

to minimize inter-channel interference due to polarization crosstalk. In case of Digital Video Broadcasting (DVB), each frequency slot contains only one modulated carrier. In the original digital satellite standard (DVB-S) the modulation is QPSK, but later standards also use 8-PSK, 16-QAM(DVB-DSNG), 16-APSK or 32-APSK (DVB-S2). From here, when we will talk about RF signals, we will be referring to this specific frequency range [9].

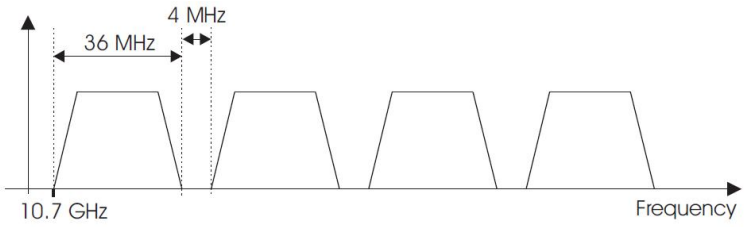

(a) Frequency slot corresponding to one transponder

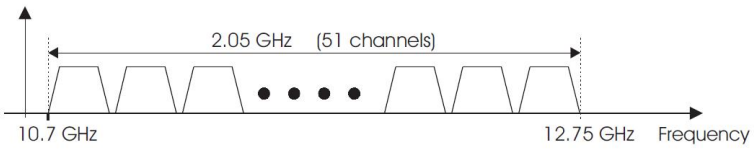

(b) Overview of the frequency slots

Figure 2.2: Frequency allocation in the K_u band

2.2 Input signal model

Every antenna element provides an input signal to the OBFN which is amplified by a Low-Noise Amplifier (LNA). When noise, interference, and channel distortion are ignored, the m-th element's signal can be written as a delayed version of the desired RF signal, $s(t) = r(t)\cos(2\pi f_{RF}t + \psi_s(t))$, as follows:

$$s_m(t) = \alpha_m r(t - T_m)\cos[2\pi f_{RF}(t - T_m) + \psi_s(t - T_m)] \tag{2.1}$$

where α_m and T_m are the amplitude weighting factor and the delay value introduced by the m-th antenna element, respectively. These values depend on the geometry of the antenna. The amplitude and phase of the signal are given by $r(t)$ and $\psi_s(t)$, respectively. In fact the desired signal consists of several subcarriers. However, it will be modeled as a standard bandpass signal with a center frequency f_{RF}.

2.3 Frequency Down Conversion

By mixing the element RF signals $s_m(t)$ with a Local Oscilator (LO), resulting in terms with frequencies $f_{RF} - f_{LO}$ and $f_{RF} + f_{LO}$. The oscillator frequency is either 9.75 or 10.6 GHz, and filtering is performed in such a way that only the terms around the Intermediate Frequency (IF) $f_{IF} = f_{RF} - f_{LO}$ in the prescribed IF range 950-2150 MHz remain. The lower boundary is there because the lower frequencies are reserved for the TV and radio signals from terrestrial broadcasting. The upper limit is caused by the transport limitations of the coax cable that is used between receiver and user. IF down conversion gives advantages also for the OBFN systems. Lower speed modulators and detectors can be used for the OBFN due to the decreased frequency. Also the bandwidth of the modulated optical signal is reduced from 2.05 GHz to 1.2 GHz, so not all the transpoders can be received, but the required bandwidth of the ring resonator-based delay elements is reduced too. Another advantage is that IF phase offsets can be corrected by simple optical phase shifts in the OBFN (which are required anyway for coherent combining). Figure 2.3 shows the spectrum before and after the down conversion.

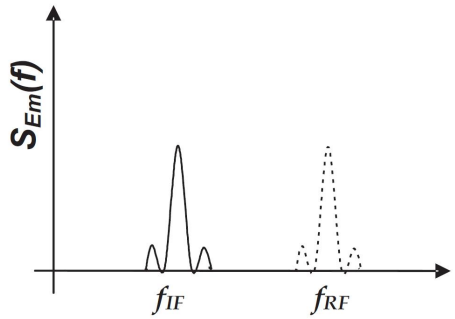

Figure 2.3: Spectrum of the RF signal (solid line) and the IF signal (dotted line)

The m-th signal, after down conversion and filtering, is given by [9]:

$$v_m(t) = \alpha_m r(t - T_m) \cos\left[2\pi\left(f_{IF}t - f_{RF}T_m\right) + \psi_s(t - T_m)\right] \tag{2.2}$$

where f_{IF} is the IF signal. For simplicity, in Equation 2.2 the same symbols for $r(t)$ and $\psi_s(t)$ are used as in Equation 2.1, even if they do not indicate the same signals, but filtered versions of these.

2.4 Electrical to optical conversion

When an OBFN is applied in a phased array receiver system, IF signals of the individual antenna element have first to be converted from the electrical to the optical domain. In order to minimize the losses, the combining of the optical signals in the OBFN should

preferably be done coherently, which requires the use of a common laser. The output light of the laser should first be split, and then modulated by the antenna element signals, using external modulators. The most straightforward way of doing this is to apply optical Double-Side Band (DSB) modulation, for example using Mach-Zender Modulators (MZMs) as shown in Figure 2.4.

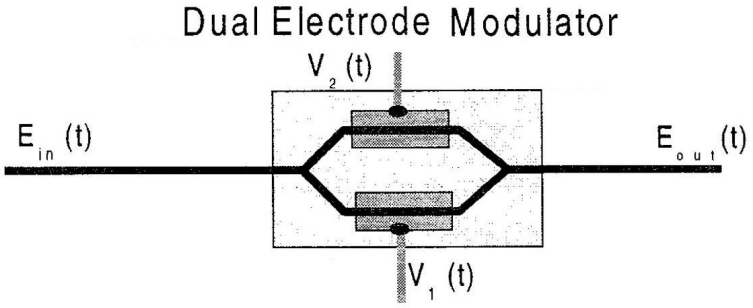

Figure 2.4: Dual electrode MZM

The working principle of the MZM is based on the difference in optical path length between the upper and lower branches. These optical path lengths can be changed by the input voltages $V_1(t)$ and $V_2(t)$ and thereby cause complete destructive or constructive interference. The output signal of the MZM is given by [10]:

$$E_{out}(t) = \frac{E_{in}(t)}{2}\left[e^{j(\pi V_1(t)+\gamma_1)} + e^{j(\pi V_2(t)+\gamma_2)}\right] \tag{2.3}$$

where γ_1 and γ_2 are the bias phases of the MZM. $V_1(t)$ and $V_2(t)$ are normalized with respect to V_π, the switching voltage of the MZM (defined as the voltage difference between complete constructive and complete destructive interference). The voltages that are applied as $V_1(t)$ and $V_2(t)$ are the IF signals. For simplification the time shifts are left out:

$$V_1(t) = a_m r(t)\cos(2\pi f_{IF} t + \psi_s(t) + \theta_1) = \frac{A}{\pi}\cos(x + \theta_1) \tag{2.4}$$

$$V_2(t) = a_m r(t)\cos(2\pi f_{IF} t + \psi_s(t) + \theta_2) = \frac{A}{\pi}\cos(x + \theta_2) \tag{2.5}$$

which have the phase θ_1 and θ_2 respectively and normalized amplitude a_m, which contains the product of the amplitude weighting factor, α_m, and the modulation index, $a_m = \mu\alpha_m$. Double-Side Band Suppressed Carrier (DSB-SC) modulation can be performed with the following phases, $\theta_1 = 0$, $\theta_2 = \pi$, $\alpha_1 = \pi$ and $\alpha_2 = \pi$. This operating point of the MZM is called push-pull [11].

A drawback for DSB modulation is the large bandwidth of the modulated optical signal. Its spectrum consists of the optical carrier and at least two sidebands. In order to avoid signal distortion in the OBFN, the optical delay elements in the OBFN should

provide flat group delay response in the entire frequency range of the modulated optical signal. As a result, alternative solutions are needed to reduce the bandwidth of the modulated optical signal.

An alternative way to reduce the bandwidth of the modulated optical signal is to remove one of the sidebands by applying optical Single-Side Band (SSB) modulation. Optical SSB modulation has been previously proposed as a means to overcome the bandwidth-limiting effect of chromatic dispersion in single-mode fiber-based Radio-over-Fiber (RoF) transmissions systems and Chirped Fiber Grating (CFG)-based optical beam forming systems.

SSB modulation needs exactly half the bandwidth with respect to optical DSB modulation. The bandwidth can be reduced even further by also removing the optical carrier, resulting in Single-Side Band Suppressed Carrier (SSB-SC) modulation, as we see in Figure 2.5. The optical bandwidth then equals the IF bandwidth. Hence, applying SSB-SC modulation significantly reduces the required number of ORRs in the OBFN, and relaxes the requirements on the sizes of the ORRs [7].

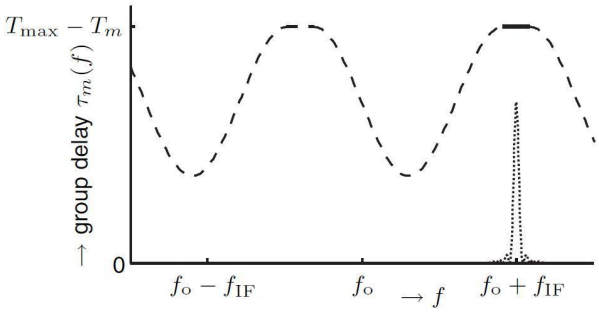

Figure 2.5: Desired group delay response from input m to the output of the OBFN in case of optical SSB-SC modulation

The way to achieve SSB-SC is making DSB-SC modulation with the push-pull operating MZM as we explained before, and afterwards filter out one of the sidebands, by means of an Optical SideBand Filter (OSBF). This OSBF is actually integrated in the OBFN chip at the output of the OBFN, making the total design easier and with a lower cost. The best optical filter in terms of intensity response, group delay response, size and number of tuning elements, is the asymmetric Mach-Zender Interferometer (MZI) with the ring resonator. We can see this OSBF in Figure 2.6 [12].

2.5 Optical Beam Forming Network (OBFN)

An OBFN is formed from optical delay elements (ORR) combined with tunable signal processing circuitry such as power splitters or combiners. UT-TE has designed a fully integrated Optical Beam Forming Network (OBFN) using a cascade of Optical Ring

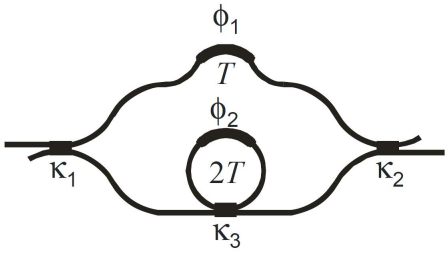

Figure 2.6: Optical sideband filter

Resonators (ORRs) as tunable delay elements. Lionix BV has designed and fabricated the optical chip. The first single-chip realization of an OBFN, based on a 1x4 binary tree topology using ORRs, was presented in [13]. Later, a 1x8 OBFN was explained in [14], [15]. Currently UT-TE is working on a 1x16 OBFN chip.
Figure 2.7 shows an ORR-based 1x8 OBFN for a transmitter phased array, based on a binary tree topology that consists of three stages with eight outputs. In this case twelve ORRs and seven tunable power splitters are used.

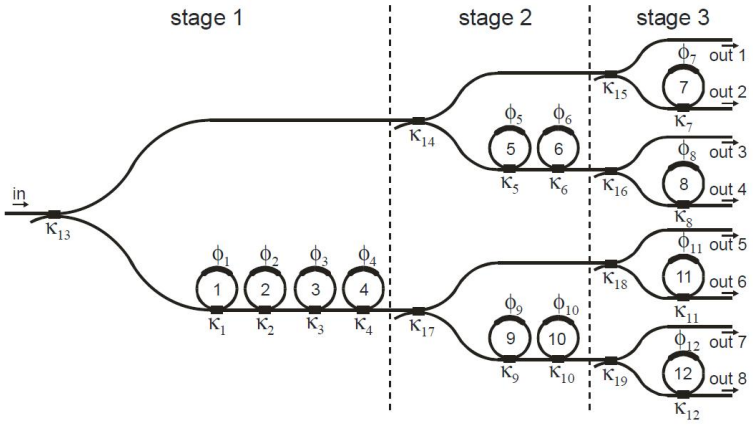

Figure 2.7: Binary tree-based 1x8 OBFN for a phased array transmitter system.

It has been demonstrated that the binary tree-based OBFN is more efficient than the parallel topology with respect to the required number of rings, therefore it has a reduced tuning complexity. Also, the binary tree-based OBFN is easy to extend because more outputs can be obtained by simply adding more stages. This extension can be showed by comparing the 1x4 OBFN in Figure 2.8 and the 1x8 OBFN in Figure 2.7.

The binary-tree receiving OBFN used in our project is presented in Figure 2.9. It consists of three stages, combining eight inputs in a single output. Each input corresponds to each antenna element of the array. Conceptually, tunable power combiners are used instead of tunable power splitters. This is where the problem to be solved in this master thesis appears.

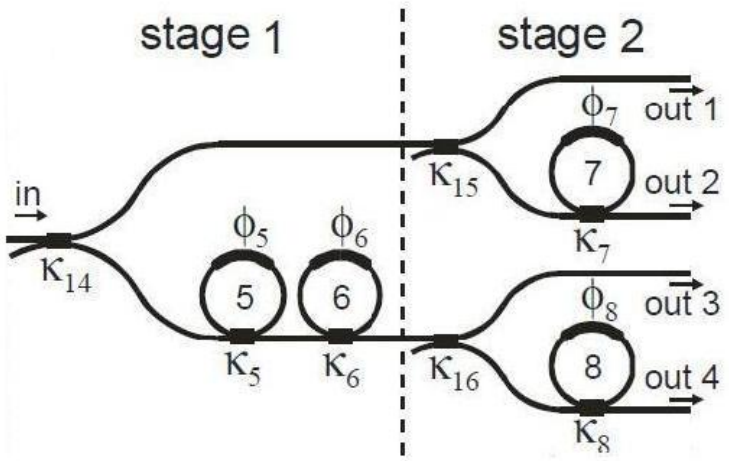

Figure 2.8: Binary tree-based 1x4 OBFN for a phased array transmitter system.

In all the points where light is combined from two branches, the optical signal has to be synchronized in order to get the maximum power at the detector. This problem only applies to the receiving system, and not to the transmitter since light is not combined. Due to different reasons, that will be explained in the following chapters, the optical signals to be combined are not synchronized, that is, are not in phase. This causes destructive interference that generates a reduction in the output power. In order to achieve optical phase synchronization, phase shifters will be used. In Figure 2.9 they are represented as black boxes in the upper branches of the combiners. The use of phase shifters is possible because of the SSB modulation prior to the OBFN: the phases of the carrier and the sideband can be independently shifted and therefore the phase offsets can be canceled by using these optical phase shifters.

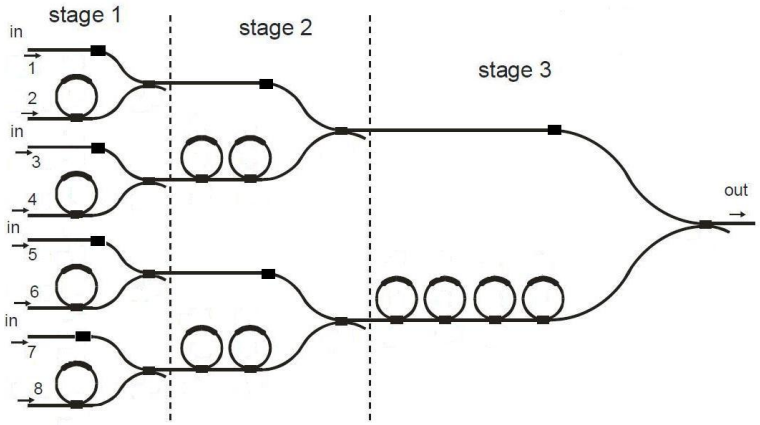

Figure 2.9: Binary tree-based 8x1 OBFN for a phased array receiver system.

2.6 Optical to electrical conversion

Finally the output signal has to be converted back to the electrical domain. An opto-electrical conversion is performed by means of balanced coherent optical detection. This configuration consists in a 2x2 coupler and two photodiodes. As we can see in Figure 2.10, in this technique the unmodulated laser signal is used to mix the signal back to IF frequency. The output signal we obtain can be written as

$$i_{out}(t) = \frac{R_{pd} P_o A_M}{2 L_s \sqrt{L_c}} r_s(t) \sin\left(2\pi f_{RF} t + \psi_s(t) + \phi\right) \tag{2.6}$$

where L_s and L_c are the coupling losses due to respectively power splitting and coupling, the photodiodes have identical responsivities R_{pd}, and the optical phases are synchronized to a common value ϕ. Balanced detection has significant advantages over single-ended detection by means of just one photodiode:

- Balanced detection cancels the DC and baseband terms that appears when we use direct detection.
- Second order InterModulation Distortion (IMD-2) is not introduced.
- The effect of Relative Intensity Noise (RIN) in the optical signal is significantly reduced, which enhaces the dynamic range of the PAA receiver.

For the previous reasons balanced detection is strongly preferred over single-ended detection.

2.7 The complete system

Once we have explained each single block, the complete optical beamformer system architecture is presented in Figure 2.10.

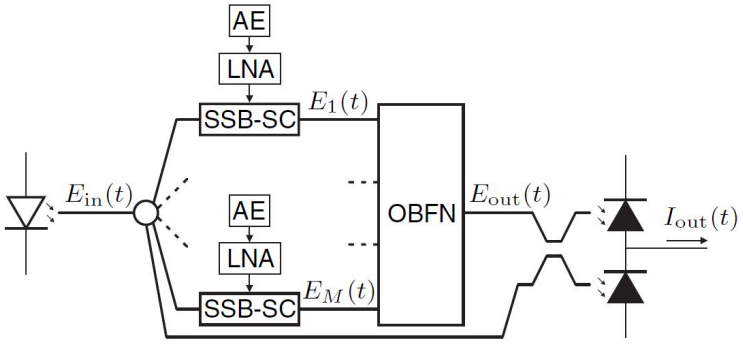

Figure 2.10: Optical beamformer architecture using optical SSB-SC modulation and balanced coherent detection

Chapter 3

Optical Phase Synchronization

The problem of the optical phase synchronization is presented in this chapter. Section 3.1 explains why optical phase synchronization is so important in our system, and why is the de-phasing problem happening. Phase shifters in the OBFN are used to solve the problem: Section 3.2 describes how to set the values of the phase shifters. The following section, presents two different solutions for optical phase synchronization. At the end of the chapter a brief summary is given in Section 3.4.

3.1 The Importance of Optical Phase Synchronization in the OBFN

In the receiver architecture (Figure 2.10) only one laser is used. Consequently, all the RF signals after the MZMs share the same carrier. For this reason, optical phase synchronization is extremely important inside the OBFN.

In Figure 2.9 we can see that the different optical modulated signals from each input are combined in the OBFN to obtain only one output. The optical inputs signals have to be combined *in phase*. The branches from the different antennas are combined two by two until we only have one output branch. Therefore when two branches are combined inside the OBFN, their optical carrier signal has to be synchronized in order to achieve maximum output signal power. The importance of synchronization can be explained easily with a simplified simulation in Figures 3.1a, 3.1b and 3.1c, where two identical signals are combined. These input signals simulate the optical carrier signals from two different branches, and the outputs represent, in turn, the output of the couplers. In Figure 3.1a, two signals in contra phase can be seen, so at the output there is no signal. In Figure 3.1b, two signals with different phase are represented, so the maximum ouput power is not obtained. Finally, in Figure 3.1c two signals exactly in phase are shown, so the maximum output power is reached.

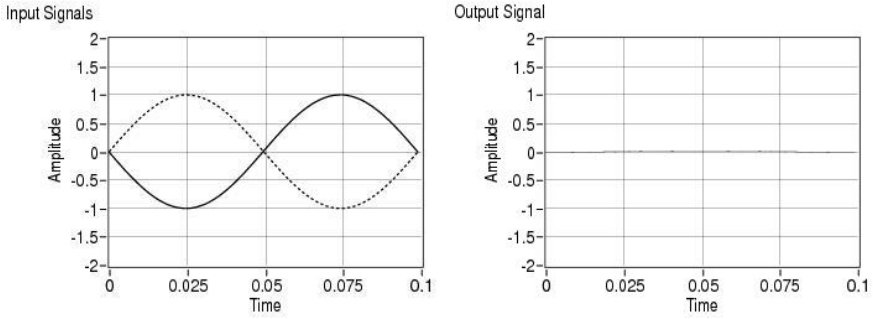

(a) Destructive Interference

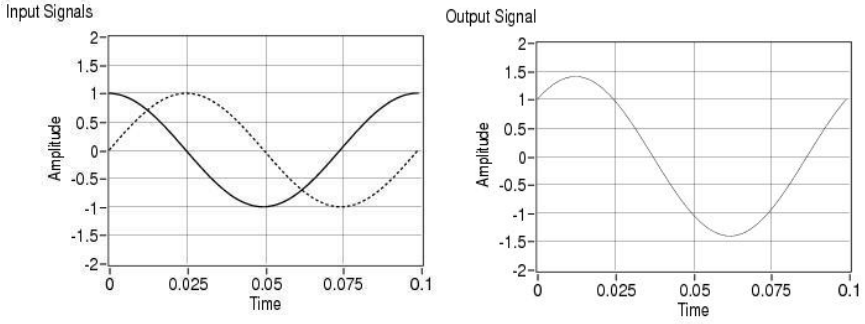

(b) Interference

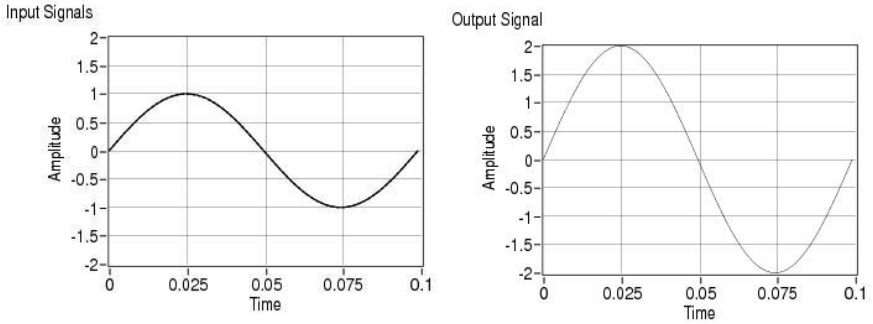

(c) Constructive Interference

Figure 3.1: Combining of two optical carrier signals

As demonstrated in Figure 3.1, when the modulated signals from two different branches are combined, synchronization at the optical wavelength level is required. In the experimental setup, only the OBFN, OSBF and carrier re-insertion coupler have been integrated on chip. The splitting and modulation of the optical carrier are done by means of fiber-based commercial off-the-self components. This is a problem for the optical phase synchronization, because it renders the optical phase very sensitive to:

- *Temperature changes:* The fiber's index of refraction depends on temperature. Changes in temperature will affect the speed of light inside the fibers and consequently the optical phase.
- *Mechanical stresses:* The application of external pressure on an optical fiber changes its properties. It induces spurious phase noise in an optical fiber.
- *Mechanical vibrations:* Vibration causes mechanical distorsions in optical fibers that induce phase fluctuations.

In order to achieve optical phase synchronization, the entire system has been built on a heavy metal plate inside a styrofoam box to minimize the temperature and mechanical fluctuations. Even though the output is more or less stabilized, drifts are still observed. Therefore, the proper behaviour of the OBFN can only be maintained stable for less than a minute.

The desired behaviour of the OBFN is achieved by the use of phase shifters. Before each coupler in the chip, a phase shifter is inserted in the upper branch, as shown in Figure 3.2. The function of these phase shifter is to adjust the optical phases in the beamformer paths in order to maximize the output signal.

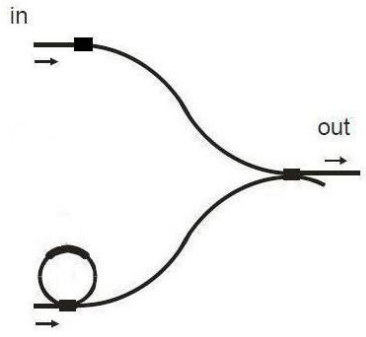

Figure 3.2: Position of the phase shifter inside the OBFN

3.2 Heater Driving System

Optical phase shifters are implemented by means of the thermo-optic effect. A heater is place over the waveguide, so when the waveguide is heated up, the refraction index changes and the optical phase shift is achieved.

A suitable heater controllersystem for the demands of the project was built by the UT-TE. The last update of the system design is presented in [16] as a consequence of the revision, integration and extension of several works are described in [17], [18] and [19]. In Figure 3.3 we can see the architecture of the control system.

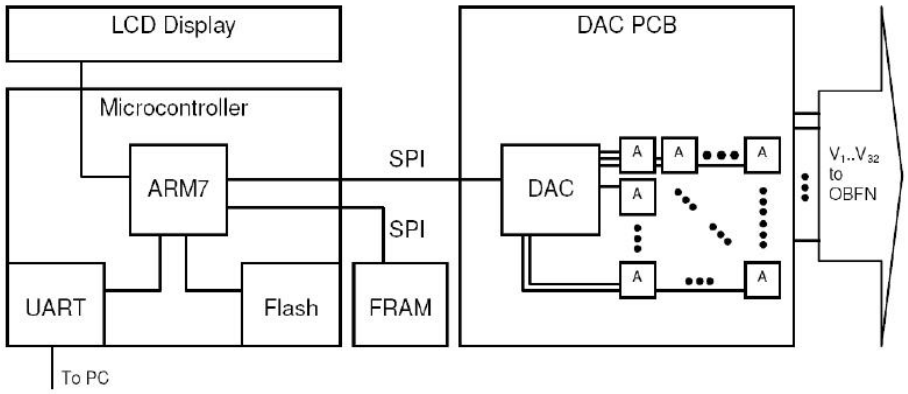

Figure 3.3: Architecture of the control system

The control system consists of a motherboard with the following elements:

- An ARM7 microprocessor, the NXP LPC2138. It runs its control software stored on the LPC2138 in flash memory. The microcontroller itself has a USB port to write this memory. The control system is able to communicate with a PC via the microcontroller's Universal Asynchronous Receiver and Transmitter (UART) interface.

- Bus architecture for stackable Digital to Analog Converter (DAC) Printed Circuit Boards (PCBs). Each DAC PCB consists of 32 channels of 14-bit resolution. Each channel is connected to an operational amplifier which boosts the voltage level six times, so that the voltage interval 0 - 30 can be addressed with 14 bit resolution. The Serial Peripheral Interface (SPI) protocol is used to communicate the microprocessor with the DAC PCB.

- A non volatile storage, a 512 Kb Ferroelectric Random Access Memory (FRAM) module from RAMTRON. It is used for the storage of tuning parameters. The SPI protocol is used to communicate the microprocessor with the FRAM.

- A connection to a PC by means of a USB to RS232 interface.

- A Liquid Crystal Display (LCD) that can be used to display some status information.

A present photograph of the system is shown in Figure 3.4.

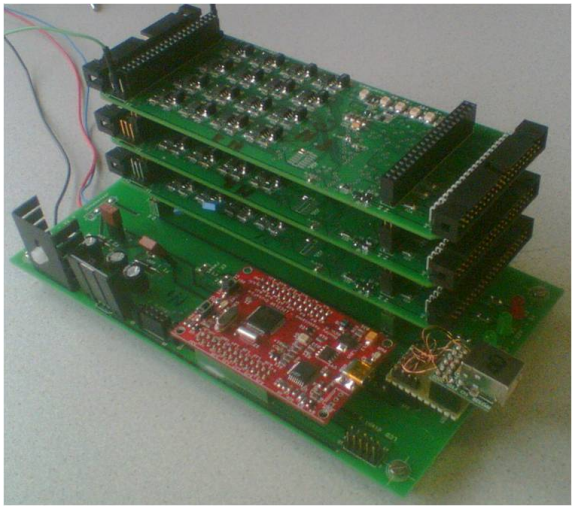

Figure 3.4: Heater driving system

Due to the specifications of our system, the heater controller has to achieve some requirements:

- *User interaction:* It should be easy for the user to set the controller, so a Graphical User Interface (GUI) was implemented to enable a user easy access to the control functions. At first, the Virtual Instrument Software Architecture (VISA) functionality of LabVIEW [20] was used for this purpose, but it was not the ideal solution from a technical point of view: some closing statements did not work as desired, resulting in 'blue screens'. Therefore, a Java interface was implemented using a Model View Control (MVC) pattern and an Observer/Observable pattern. Its GUI is shown in Figure 3.5. It consists in slider bars to set the channels of the controller to a specific value. The range of the slider bars vary from 0 to 3000 in one unit steps, representing the 0-30 V range. This means that the resolution of each channel is 10 mV. In addition, with this program the tuning settings can be stored and loaded again [16].

- *Speed:* Settings should be completed much sooner. The Java GUI is event-based, this makes channels change faster [16].

- *Extendability to more channels:* A single DAC PCB can only handle 32 channels and for the FlySmart chip, 38 channels need to be controlled. To solve this problem, the possibility of extending the number of connected DAC PCBs is needed. A solution is implemented making use of the bus structure of the PCBs,

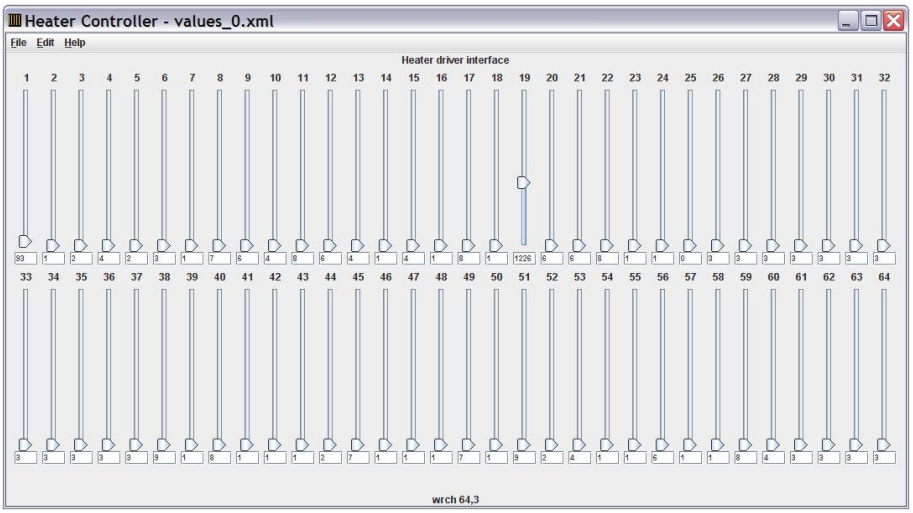

Figure 3.5: Java GUI for setting the controller

to stack them on top of each other. For this purpose, extra wiring and driver modifications were added to drive up to three DAC PCBs, enabling the controlling of 96 channels of 14-bit each. For the FlySmart chip only two DAC PCBs are needed.

- *Setting calculation:* This version of the controller is able to calculate voltages, when phase shifts and coupling numbers are given by the user.

3.3 Optical Phase Synchronization: Solutions

In this section two different techniques to achieve optical phase synchronization are described: phase-corrected frequency dithering technique, using external signals inside the OBFN to synchronize the optical phase, and signal power technique, using the measure of the RF output power of the OBFN as an indicator. Both solutions stabilize the output signal actively by means of a feedback loop.

3.3.1 Phase-Corrected Frequency Dithering Technique

Frequency dithering techniques were proposed within the framework of coherent Optical Code Division Multiple Access (OCDMA) techniques [21]. The technique consists of inserting small harmonic (dithering) signals, each one with a different frequency, in the OBFN. These signals are superimposed to the input signals of the MZM, so that the output of the OBFN the signal contains additional signals. Then, using Lock-In Amplifiers (LIAs) and Proportional-Integral-Derivative (PID) controllers, the new contributions can be distinguished and the phase shifters can be adjusted properly. The scheme can be seen in Figure 3.6.

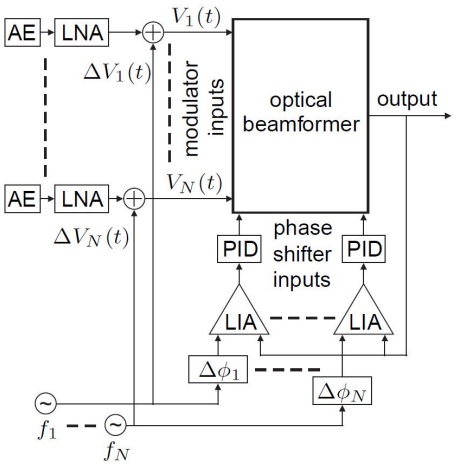

Figure 3.6: Optical phase-locking scheme using frequency dithering and a feedback loop

The frequencies of the dithering signals should be in same frequency range that the OBFN is intented to be used. Besides, these signals must not corrupt the information signals. It can be done due to the well-defined relation between the dithering signals at the ouput and the phase transfer of the OBFN in the frequency range of interest [22].

3.3.2 Signal Power Technique

The purpose of the optical phase synchronization is to obtain the maximum signal power at the output of the OBFN: this technique is based on this concept. The output power of the OBFN is used as an indicator of the degree of synchronization of the optical phase.

The principle consists on an external circuit constantly measuring the output and changing the phase shifters accordingly, until the maximum ouput power has been reached. This solution does not insert new signals into the OBFN like the dithering technique. Therefore, possible interferences between the antenna signals and the small harmonic signals do not appear.

In conclusion, phase synchronization by maximizing the output signal power is less complex than phase-corrected frequency dithering technique but its effectiveness might not be the same with all the modulation techniques. The following chapters of this Master Thesis are focused on the measured signal power technique.

3.4 Summary

The problem of the optical phase synchronization and a solution were presented in this chapter. The reasons why this phenomenon is happening in our system and the importance of the synchronization were discussed in Section 3.1. After that, how to change the phase shifters by means of the heater controller was explained in Section

3.2. Possible solutions were presented in Section 3.3, and finally the chosen solution has been explained in Section 3.3.2.

Chapter 4

Design of the Feedback Loop

The optical phase synchronization is achieved by maximazing the output signal power of the OBFN. This chapter describes the feedback loop for the optical phase synchronization. Firstly, the requirements needed for the feedback loop are presented in Section 4.1. The feedback loop diagram is introduced in Section 4.2 and explained in Section 4.3.

4.1 Requirements

In this section the requirements for the feedback loop are presented. The features required for the system are introduced and explained below:

- *Speed:* The total speed of the system will be the time needed to measure the power, to calculate the new value of the phase shifter and to send the command to the heater controller. The system should be fast enough to continuously maintain the maximum ouput power. Since our system will be used for antenna arrays of hundreds of elements (N), the feedback loop has to change $N-1$ phase shifters before the ouput power fades. For this reason, the speed of the feedback loop is extremely important.

- *Accuracy:* The phase shifter values are calculated based on the RF power, so the accuracy of the power measurement is very significant.

- *Size:* The feedback loop should be compact. The system will be used in airbone applications, where size and weight are really important. The feedback loop system's size should be comparable to the OBFN's size.

- *Interface:* The designer needs information about the running system. For this reason the system should have an interface by means of Light Emitting Diodes (LEDs), a display, or another device.

- *Price:* The system should be as cheap as possible. For this purpose is desirable to use low cost off-the-shelf components.

4.2 Feedback Loop Block Diagram

As explained in Section 3.3.2, a feedback loop is used to synchronize the optical phases. This feedback loop measures the signal power at the output of the OBFN, and based on this parameter, communicates with the heater controller to properly set the values of the phase shifters. The scheme of the complete system with the feedback loop is shown in Figure 4.1.

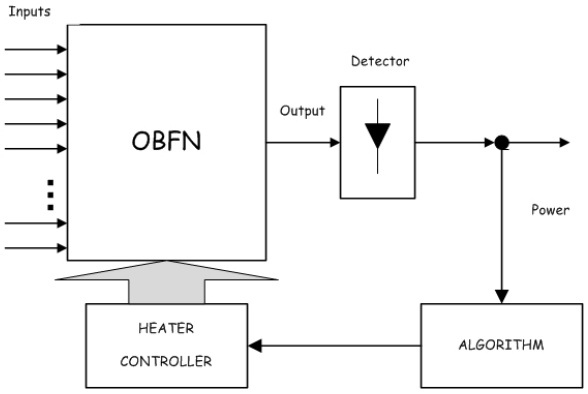

Figure 4.1: System with the feedback loop

The operation of the feedback loop is explained below:

1. **Measure the signal power:** First of all the RF signal is measured. This step is really important because the new value for the phase shifter is based on this signal power measure.

2. **Algorithm:** The algorithm calculates the new phase shifter value, using the power as input. The algorithm has to calculate the new value for the phase shifter in order to reach the maximum power in the shortest number of steps as possible.

3. **Change the Phase Shifter:** Finally, the feedback loop has to change the phase shifter value. As explained in the previous chapter, a heater driving system has been implemented, so the feedback loop has to send the correct command to the heater controller. This device will properly set each phase shifter to its corresponding value.

The feedback loop is running continuosly. After changing the phase shifter in step 3, the feedback loop starts again from step 1. This can be shown in the block diagram of the feedback loop in Figure 4.2.

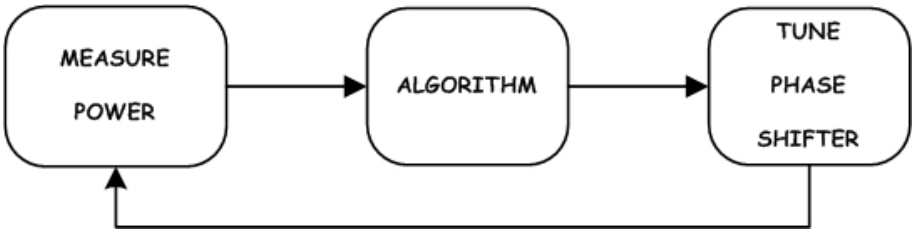

Figure 4.2: Hill Climbing Block Diagram

4.3 Design

In this section, the actual design of the optical phase synchronization system is presented. Before implementing the feedback loop on a PCB board, we want to demonstrate that the signal power technique is successfully working. For this reason in this Master Thesis the feedback loop is implemented through a PC. The design of the feedback loop is explained in the next subsections.

4.3.1 Measuring the RF Power

The feedback loop measures the power at the output of the OBFN. Before the best implentation was reached, different options were studied.

PC Television Card

The first option studied is using a Peripheral Component Interconnect (PCI) DVB receiver card for a computer as signal quality/level indicator. After the OBFN, the optical signal is converted in the IF DVB signal by the detector, so that this signal can be connected directly to a PCI DVB receiver card. Consequently, the power of the DVB signal can be measured by means of the software used to watch television on the PC. Most DVB receiver softwares to watch television has an interface to show the level and the quality of the signal, as shown in Figure 4.3. The idea is to obtain those parameters provided for the program as binary data. Afterwards, this data will be the input of our feedback loop.

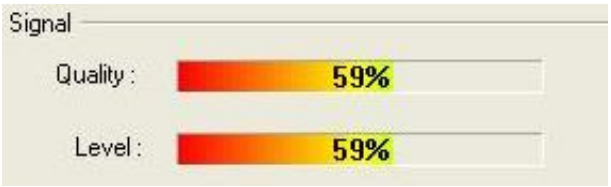

Figure 4.3: Software Freeware progDVB. PCI card cost: 120 euros

At the end of the research the conclusion is that using the PCI card is a complex option: the software available only offers a graphic interface to show the power and the

quality of the signal by means of bars, while it does not offer a function to export the values on the bars to binary data. In order to obtain this binary data from the program, is necessary a deep research on the program's source code. Besides the difficulties of finding the source code, the effort required, is beyond the scope of this master thesis.

Power Meter

After this research, a new option is studied. This option is based on the use of a power meter like the ones used by the satellite technicians to align the dish main beam to the satellite. These devices have an interface that shows the power of the RF signal. The problem with these devices is the same as before, obtaining the parameter in binary data is not straightforward, and would require a hardware modification and an ADC. This power meter can be seen in Figure 4.4.

Figure 4.4: Power meter used to find the satellite. Cost: 20 euros

Following with the research, there are some power meters in the market that can connect with the PC through an USB port. As a result, it is possible to obtain the power and the quality of the signal in binary data. The device is shown in Figure 4.5. The problem is, in this case the high price of the device.

Figure 4.5: Power meter with USB connection. Cost: 700 euros

Electronic Instrumentation

The study follows using advanced electronic equipment avilable in the laboratory. The first choice is to use an spectrum analyzer. A picture of the instrument used is shown in Figure 4.6. By means of this instrument the RF power can be easily measured.

The spectrum analyzer provides several interfaces: LAN connection, USB connector, General-Purpose Instrumentation Bus (GPIB) interface and a screen where the spectrum of the RF signal can be seen. The interface that was used for the project is the GPIB. The main advantage of this interface is the speed of the data rate, about 8 MB/s. By means of this connector the device can be controlled by a PC and consequently, the RF power can be obtained easily in binary format. Another advantage is that the power of a single transponder can be measured.

Figure 4.6: Agilent N9020A-526 MXA Signal Analyzer (20 Hz to 26.5 GHz). Cost: 40.000 euros

After the spectrum analyzer, the option of using an RF Power Meter is compared, in terms of adquisition speed. The Agilent E4417A EPM-P Series Dual-Channel Power Meter is shown in Figure 4.7. This Agilent Power Meter also provides GPIB connection as the spectrum analyzer. The problem is that this instrument appears to be slower in measuring the power than the spectrum analyzer.

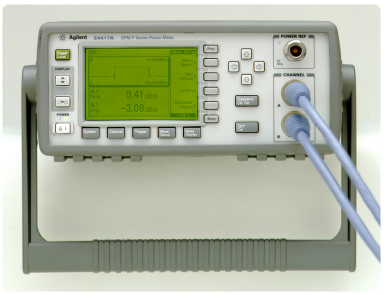

Figure 4.7: Agilent Dual channel EPM-P series power meter. Cost: 20.000 euros

The conclusion of the research is that the spectrum analyzer is the best solution with respect to the requirements to measure the RF signal power. Therefore, the spectrum analyzer was chosen as part of the feedback loop.
As explained before, the RF signal measured is the DVB signal received from the satellite. The bandwith of this RF signal is down converted to IF signal from 950 MHz to 2150 MHz. Instead of measuring all the IF signal, the bandwith to measure for the spectrum analyzer will be the transponder in the middle, 36 MHz. The result will be the same if the transponder in the middle is maximized, or if the whole bandwidth is. For this purpose the measurement of the spectrum analyzer is configured as: “Channel

Power". To measure that bandwidth the center frequency is set at 1.545 GHz and the bandwith of the channel to 36 MHz.

4.3.2 Setting the Phase Shifters

Once the power of the signal is measured, the phase shifters have to be set in order to achieve the maximum RF power. As said before, the number of phase shifters is $N-1$, where N is the number of antenna elements. Hence, the feedback loop has to set $N-1$ phase shifters. The aim of the feedback loop is to achieve the global maximum output power by tuning all the phase shifters. The new value of each phase shifter is calculated by an algorithm implemented on a PC. In the next Chapter, the study and the implementation of this algorithm will be discussed in detail.

4.3.3 Communicating with the Heater Controller

Finally, the new values calculated for the phase shifters have to be sent to the heater controller. As explained in Section 3.2, the heater driving system has a connection to a PC using USB, via the UART of the microcontroller. It means that to close the feedback loop the PC is connected to the heater controller through the USB port over RS232.

4.3.4 Software on PC

In order to implement the feedback loop, a software running on a PC is needed. This software has to communicate with the hardware of the computer and run the algorithm to calculate the phase shifters. For this reason, LabVIEW software is used. LabVIEW contains different blocks to communicate with the hardware.

Communicating with the Spectrum Analyzer National Instruments, the company that developes LabVIEW, support the users with drivers to control the instruments. Once the driver for the spectrum analyzer used is installed in LabVIEW, is easy to interact with the instrument by means of specific blocks. The LabVIEW front panel to configure the Spectrum Analyzer is shown in 4.8.

Running the Algorithm Labview offers scripts to be inserted in our file. The algorithm is implemented in Matlab and inserted in Labview by means of a Matlab script. The Labview front panel to configure the algorithm and see the results is shown in 4.9.

Communicating with the Heater Controller For this purpose the VISA functionality of Labview is used. Our labview program sends a plain text command to the

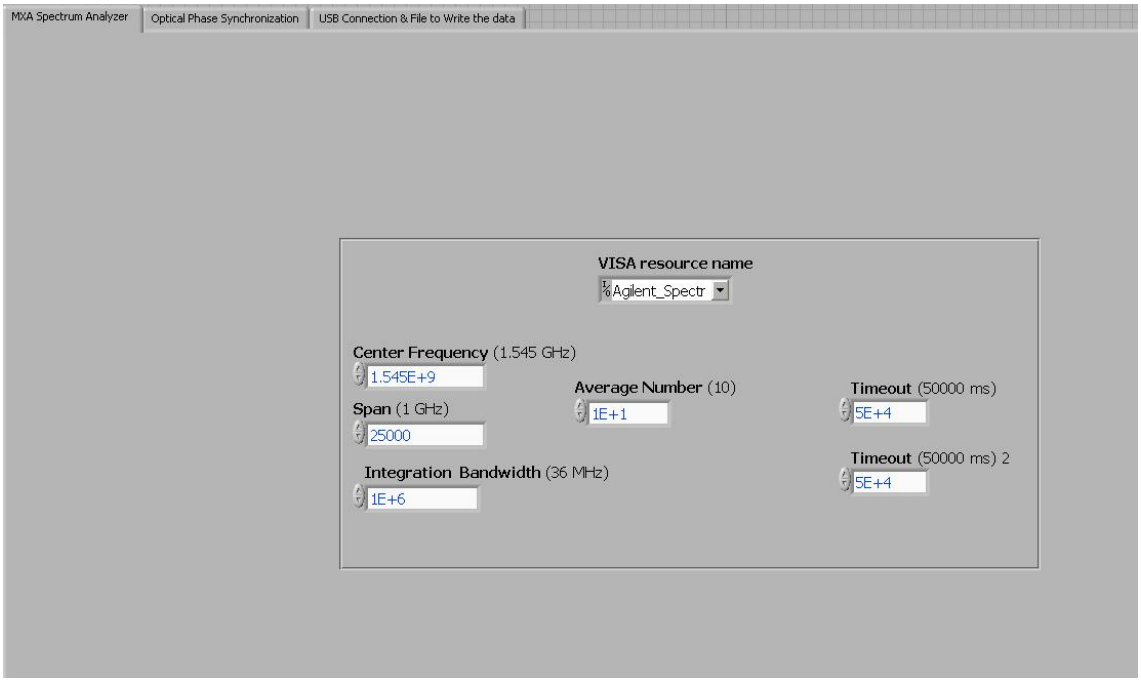

Figure 4.8: Labview Front Panel for the Spectrum Analyzer

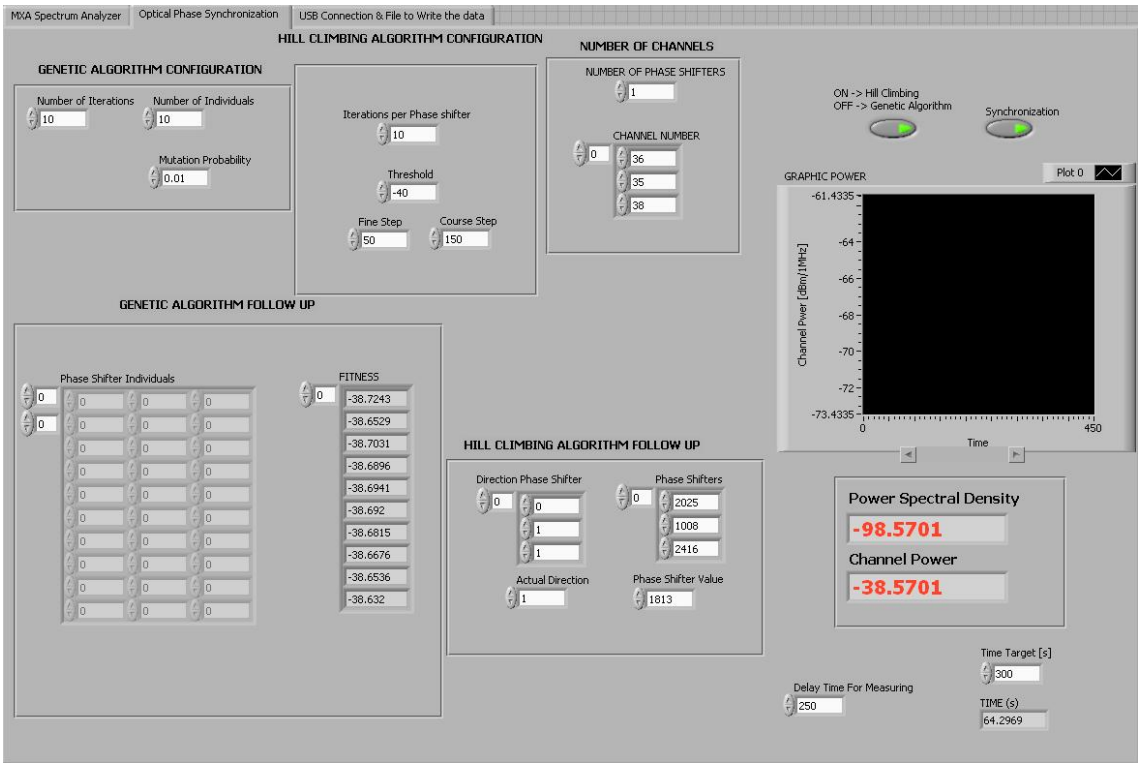

Figure 4.9: Labview Front Panel for Feedback Loop Algorithm

controller using RS232. The command to send that sets the value of the phase shifter is: "wrch number, value". The Labview front panel to configure the connection to the heater controller and the file to save the results is shown in 4.10.

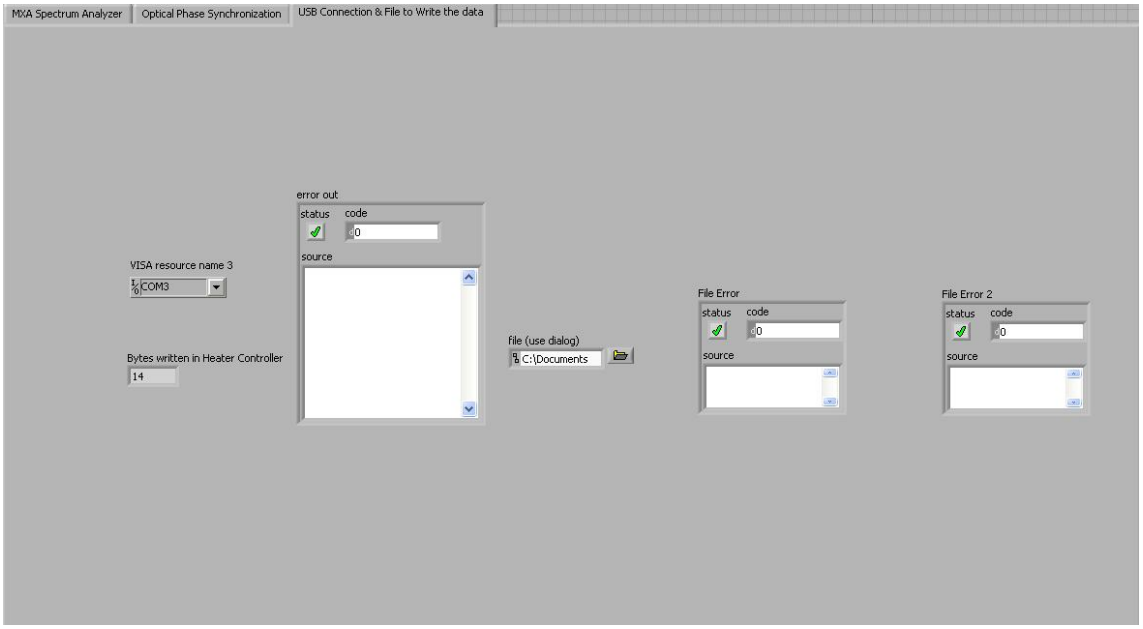

Figure 4.10: Labview Front Panel to configure the connection to the Heater Controller and the File to save the results

4.4 Summary

After studying the requirements and the diagram of the system, the design of the feedback loop is presented. The feedback loop implemented after the research is shown in Figure 4.11.

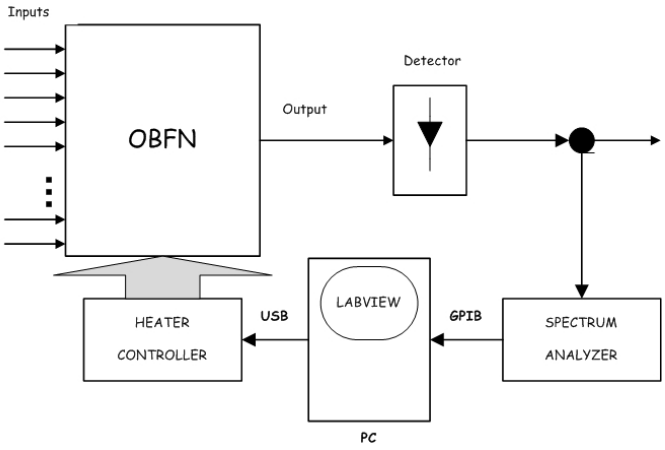

Figure 4.11: Feedback Loop implemented in the laboratory

Chapter 5

Implementation of the Algorithm

Previous chapter explained the design of the feedback loop. The loop has to measure the RF power and communicate with the heater controller, but the core of the feedback loop is its algorithm.
This Chapter discusses the process of the implementation of the algorithm for the feedback loop. During this Master Thesis different algorithms were studied until deciding the best algorithm for our system. In Section 5.1 a local search method is explained, the Hill Climbing algorithm. Next Section, 5.2, explains a global search method, the Genetic Algorithm. Finally, in Section 5.3 the algorithm implemented for the feedback loop is explained. To conclude the chapter, a summary is presented in Section 5.4.

5.1 Hill Climbing Algorithm

Due to its easy implementation, the study starts with a local search algorithm, Hill Climbing Algorithm (HCA). This algorithm uses a technique of mathematical iterative optimization. Although more advanced algorithms may give better results, in some situations HCA works just as well.

5.1.1 Hill Climbing Parameters

HCA has some parameters that have to be set at the initialization. Those parameters are explained below:

- *Threshold Power:* The output power has to be higher than this desired value.
- *Course Step:* Parameter to move the phase shifter fast.
- *Fine Step:* Parameter to move the phase shifter slow. This is the default step to move the phase shifter.

- *Direction of the Phase Shifters:* The operation to change the value of the phase shifter is similar to the graphic slider bars. For this reason, an initial direction to move the phase shifter has to be set at the beginning. The direction chosen for the first iteration is the right.

5.1.2 Hill Climbing Methodology

As explained in Chapter 4, the algorithm calculates the new value of the phase shifter based on the output RF power. The flow diagram implemented in the feedback loop is shown in Figure 5.1. The algorithm changes the value of the phase shifters in order to reach the maximum power. HCA works cyclically: first tunes one phase shifter a number of iterations, and after that, starts tuning the next phase shifter. Once all the phase shifters are tuned, the algorithm starts again with the first phase shifter. The methodology of the HCA is explained below:

1. **Initialization:** First, the parameters are initialized to the proper values. All the phase shifters are initialized to random values. These values are not yet sent to the real phase shifters.

2. **Set the phase shifter to be tuned:** The next step is to set the phase shifter that is going to be tuned.

3. **Set the value of the phase shifter:** The value of the phase shifter is sent to the heater controller.

4. **Measure the output power:** The ouput power obtained with the new value of the phase shifter is measured.

5. **Compare the power with the threshold:** If the power is lower than the threshold, it means that the phase shifter value is far from the optimum, so it, should be moved faster to achieve the maximum power more quickly. Therefore, the course step is set.

6. **Compare the actual power with the power before:** At this point, the power obtained with the current phase shifter value is compared with the power obtained before. If the current power is more than the one before, this means that the direction is the correct one, so the phase shifter will continue to move in this direction. If not, the phase shifter will change its direction and come back to the previous value.
   The implementation of the heater controller makes the phase shifters to range from 0 to 3000. The movement implemented for the phase shifters is cyclic. When the phase shifter value is higher than 3000, it will start again from 0; and when is lower than 0, it will start from 3000.

7. **Check number of iterations:** If the total number of iterations has been reached, the algorithm continues from step 2. If not, the algorithm continues from step 3.

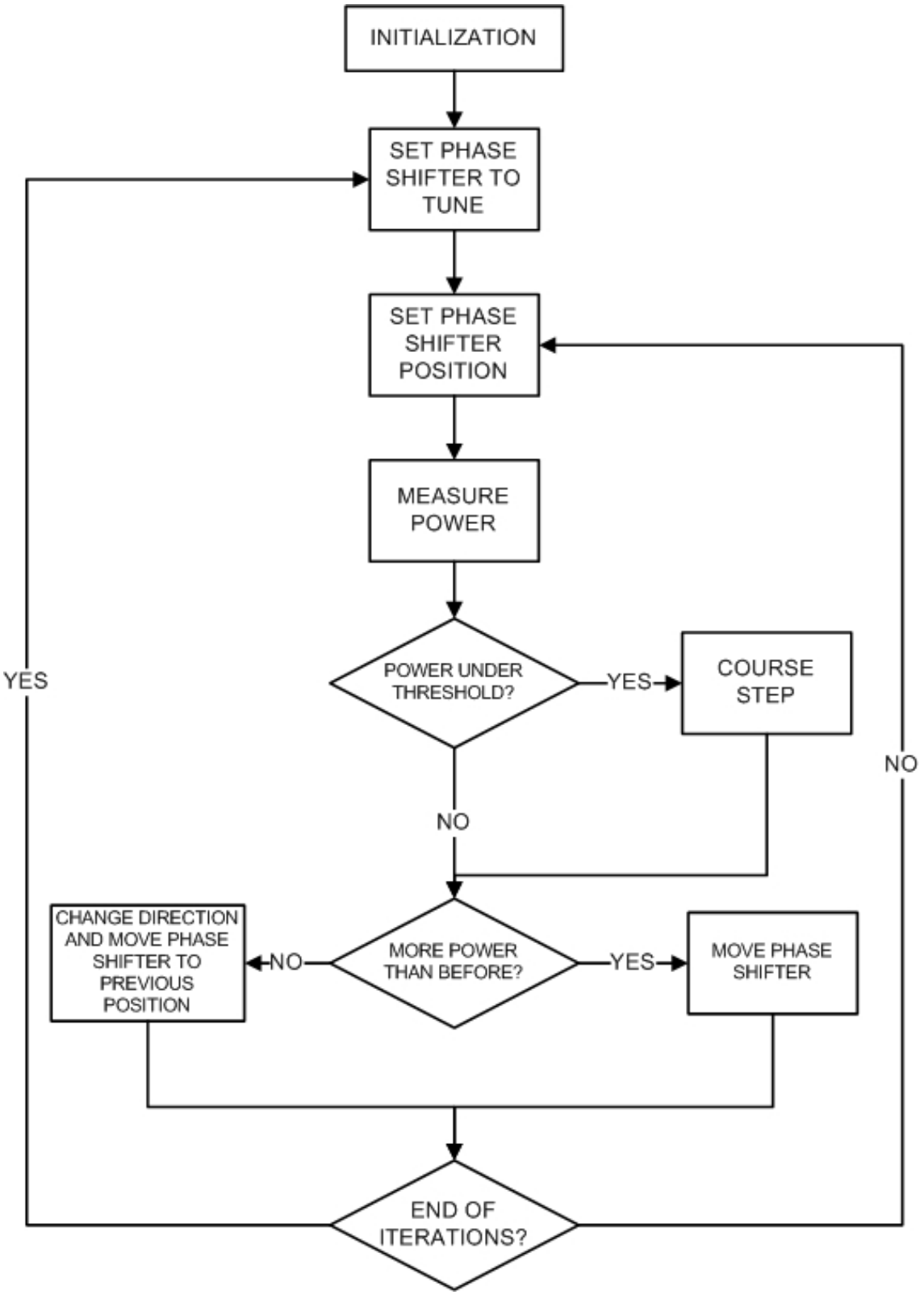

Figure 5.1: Hill Climbing Algorithm Flow Diagram

5.1.3 Hill Climbing Limitations

The main problem of the HCA is that the current solution could be close to optimal, but it is not guaranteed that HCA will ever come close to the global maximum. The algorithm could get stuck in some states that are not the goal, as shown in Figure 5.2. The cases where Hill Climbing algorithm does not find the maximum output power are:

- *Local maximum:* The output power for the actual positions of the phase shifters is higher than close positions of the phase shifters, but it does not mean that the global maximum has been reached.
- *Plateau:* Occurs when we get to a "flat" part of the search space. This corresponds to close positions of the phase shifters where the power is the same. This kind of flatness can cause the algorithm to cease progress and wander aimlessly.
- *Ridge:* This case is a special kind of local maximum. A ridge is a curve in the search place that leads to a maximum, but the orientation of the ridge compared to the available movements that are used to climb is such that each move will lead to a smaller point. In other words, each point on a ridge looks to the algorithm like a local maximum, even though the point is part of a curve leading to a better optimum. It is impossible to pass with fine steps.

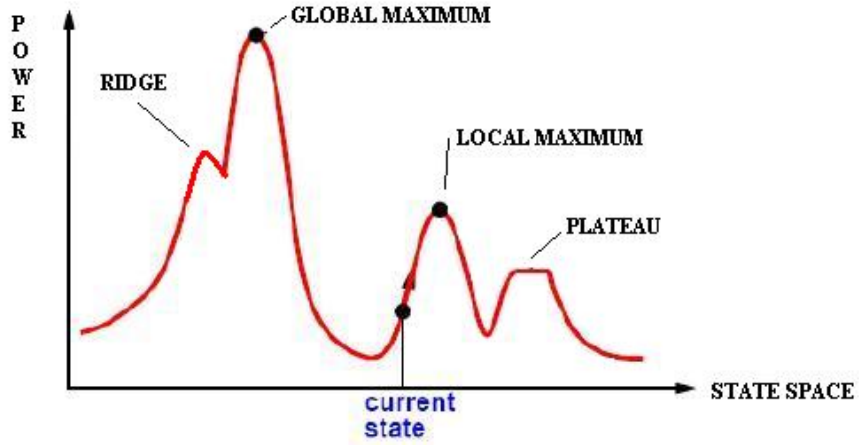

Figure 5.2: Hill Climbing Problems

In conclution, the HCA is not an efficient algorithm for our feedback loop. With a 2x1 OBFN, this algorithm is valid because the output power when the two branches are synchronized, only has one maximum. The problem is when a Nx1 OBFN is going to be synchronized. Now, the number of phase shifters is $N-1$, and depending on the synchronization of each branch, the output could have several local maximums that

perform an incorrect synchronization. Hence, the Hill Climbing algorithm could get stuck in any of these local maximums and never perform the correct synchronization where the global maximum is reached.

5.2 Genetic Algorithm

In this section, a global search algorithm is presented, a Genetic Algorithm (GA). These kind of algorithms are a particular class of evolutionary algorithms proposed by John Holland in the 60's [23]. GAs use techniques inspired by evolutionary biology such as inheritance, mutation, selection, and crossover.

5.2.1 Genetic Algorithm Methodology

Genetic algorithms are implemented as a computer simulation in which a population of candidate solutions (called individuals) evolves toward better solutions. The operation of the HCA for the feedback loop is explained below:

1. **Initialization:** The algorithm starts generating a population of M individuals. Each individual represents the configuration of all the phase shifters (N) in the OBFN.
   The representation of each individual is a binary bit string. As said, the phase shifters vary from 0 to 3000 in decimal format, so to encode the value of the phase shifters in binary, 12 bits are needed. Therefore, to represent one individual, all the phase shifters are concatenated in binary format. Then, the number of bits used for each individual is Nx12.

2. **Fitness:** In each generation, every individual is evaluated. As explained before, one individual is formed by all the values of the phase shifters in the OBFN. For each individual, all the phase shifters have to be set, and after that, the ouput power is measured.

3. **Selection:** A subset of the existing population is selected to breed a new generation. This selection is based on the fitness. The half of the individuals of the population which have the best output power are chosen.

4. **Reproduction through crossover:** The next step is to create the next generation. The binary individuals selected are crossed over in pairs at a randomly chosen point.

5. **Mutation:** Any of the bits of the new individuals can be randomly mutated, with a probability depending on the mutation rate.

6. **Check number of iterations:** The algorithm terminates when a fixed number of generations has been produced.

7. **Set best individual:** When the algorithm stops, the best individual of the generation is set in the OBFN.

The methodology and the flow diagram implemented for the GA feedback loop can be easily seen in Figures 5.3 and 5.4, respectively.

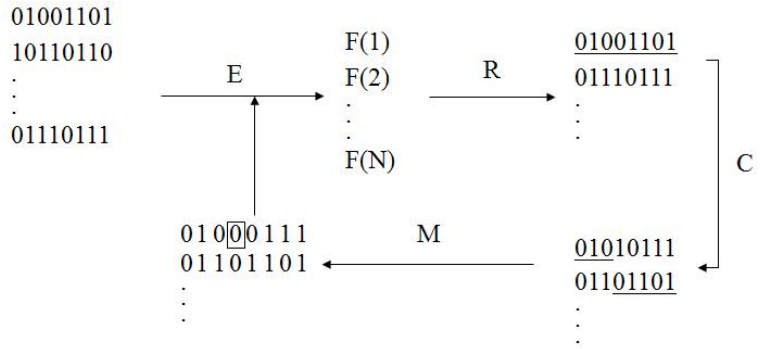

Figure 5.3: Genetic Algorithm. E = Evaluation of the Individuals. R = Reproduction. C = Crossover. M = Mutation.

5.2.2 Genetic Algorithm Limitations

Despite this algorithm calculates the phase shifter values needed to achieve the global maximum output power, the GA does not offer tracking. This means that after running the algorithm, the values of the phase shifters are correctly set to obtain the global maximum power, but if the output power goes down due to desynchronization, to achieve again the maximum power, the algorithm has to start from step 1 and this is unefficient. It means that the maximum power might not achieved continuosly, which is unacceptable for receiving a DVB signal continuosly with good quality.

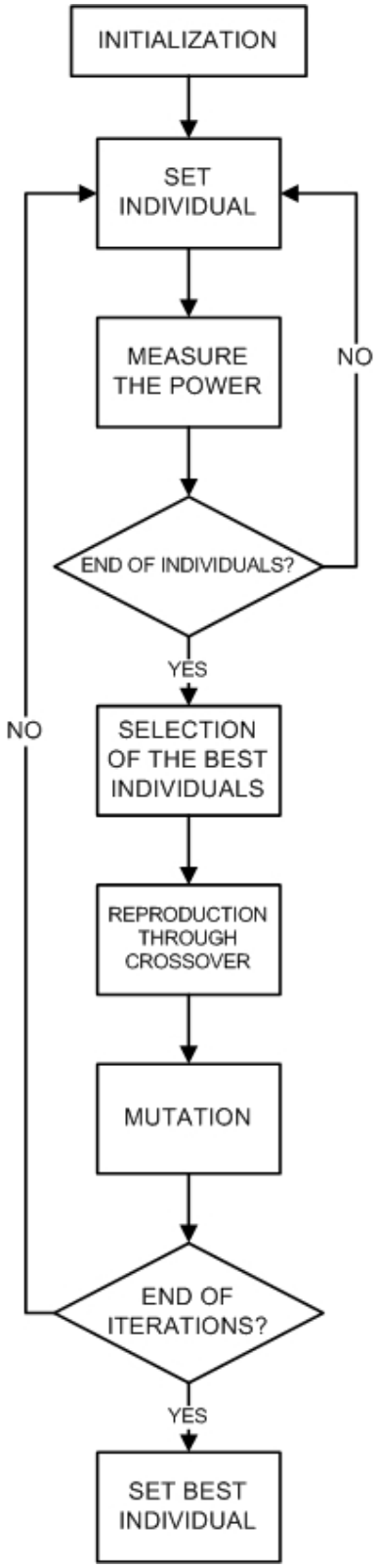

Figure 5.4: Genetic Algortihm Flow Diagram

5.3 Algorithm Implemented in the Feedback Loop

After studying the local and global search algorithms, their limitations for the application to our system have been explained. In this Section, the algorithm chosen to be implemented in the feedback loop is presented.

The algorithm has to solve the problems of the previous algorithms. The solution is to combine local searches with global searches in order to use their advantages and counteract their limitations. The algorithm implemented is a combination of both:

1. **Genetic Algorithm:** First the GA is executed. After this, the global maximum power is reached.

2. **Hill Climbing Algorithm:** Once the GA is executed, the HCA starts. The values of the phase shifters calculated by the GA are used as starting point by the HCA. This algorithm offers tracking, so if the ouput power is decreasing the algorithm will keep the power in the global maximum just changing the position of the phase shifters one by one, cyclically.

5.4 Summary

The implementation of the algorithm for the feedback loop was presented. The chapter discussed the local search algortihm HCA, and the global search algorithm GA. Due to the limitations for the system presented by these algorithms, a new algorithm has to be used. Finally, the algorithm actually implemented is a combination of both algorithms.

Chapter 6

Measurements

This Chapter describes the measurements of the feedback loop conducted on an 8x1 OBFN. The following Section 6.1 describes the setup of the system used for the measurements. Then, in Section 6.2, the feedback loop is tested using an RF tone as input. Finally in Section 6.3 the feedback loop is tested for the DVB signal. This Chapter closes with conclusions on the measurements in Section 6.4.

6.1 Measurement Setup

Once the research for the feedback loop has come to its final implementation, the algorithm has to be tested. A 8x1 OBFN chip is used to test the feedback loop. The tests are started by gradually increasing the system complexity: in this Master Thesis, only two inputs (numbers 1 and 2) and one ouput (number 8) of the chip have been used. This output corresponds to an output of the OBFN without the OSBF.
The implemented setup is simulating the reception of a planar front wave RF signal with a 2x1 OBFN. It means that one signal on an antenna element is not delayed in comparasion with the other. For this reason, inside the OBFN no delays are needed to combine the signals, so the ORR branch 2 is not used. Since only two inputs are combined, only one phase shifter, the one in branch 2, is tuned by the algorithm in order to synchronize the optical phase. The setup used for the measurements is shown in Figure 6.1.

6.1.1 Setting the Laser

The laser used on the system is an EM4 high power Distributed FeedBack (DFB) laser: it offers high power, low RIN and stable phase modulation properties. The DFB laser device is hermetically sealed into an industry standard 14 pin butterfly metal- ceramic package. The model used, the EM253-080-057, can offer 100 mW of output power with a wavelength of 1551.72 nm. Since for this setup the ORRs are not used, it is not

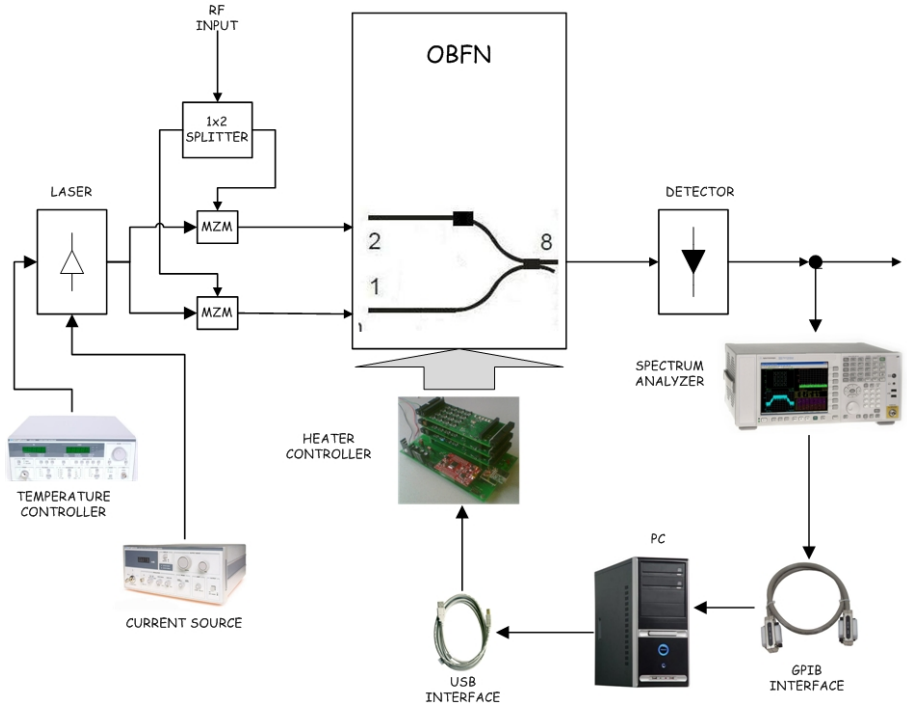

Figure 6.1: Setup Layout

crucial that the wavelength of the laser is tuned in order to match the ORRs band. Also the OSBF is not used.

The output power of the laser depends on its temperature and bias current. First of all, the temperature of the laser has to be controlled. For this purpose, the ILX Lightwave LDC-3724 Laser Diode Controller is connected to the laser. The temperature controller is set to 30 degrees centigrades.

Once the temperature is stabilized, the output power of the laser will be set to the desired value by controlling the bias current. For this purpose, the ILX Lightwave LDX-3620 Ultra Low Noise Current Source is used. To set the output power of the laser to 20 dBm, the output of the laser is connected to the lightwave multimeter, HP 8153A, using the optical module sensor HP 81532A. The maximum input power of the optical sensor is 12 dBm, so the laser can not be connected directly to the power meter. The steps to set the ouput power of the laser are explained below:

1. The laser power is set to the maximum value that can be measured with the power sensor, 12 dBm. The laser current for this output power is 100.9 mA.

2. The laser is connected to an optical attenuator, the ANDO AQ-3105. First, the insertion loss of the attenuator has to be measured. The attenuator is set to zero and its output is connected to the power sensor. Now the power is 9.9 dBm, so its insertion loss is 2.1 dBm.

3. The attenuator is set to 10 dBm. Then the output power of the laser is:

$P_{powermeter} = P_{LASER} - L_{att} - L_{ins}$. To have a laser output power of 20 dBm, the power sensor after the attenuator has to measure 8 dBm. The laser current for 20 dBm output power is 410 mA.

6.1.2 Setting the Modulators

After setting the laser, the next step is to tune the optical modulators. The Avanex Powerlog FA-20 Analog Intensity Modulators are used in our system. Their frequency range covers from DC to beyond 20 GHz with a very smooth frequency response. These modulators are used due to their high linearity combined with an exceptional low drive voltage and a small footprint. The type of modulation provided for the modulators depends on the bias point. The procedure to tune the modulators is shown below.

1. As RF input to the modulators we use a 0 dBm tone at 1.545 GHz, as shown in Figure 6.2.

2. To set the bias voltage, we look at the optical power. The optical input power comes from the common laser source that is split in eight to feed all the modulators. The output of one modulator is then connected directly to the optical power meter. The bias voltage applied to the modulators at the beginning is zero. Then the voltage is increased until the maximum optical power is reached. After that, the modulator is set to the 3 dB point: in this bias point, the third order intermodulation is kept to the minimum.

6.1.3 Tuning the Combiner

Once the modulators are set, the last step is to combine properly the signals. In order to tune the combiner, the Java interface for the heater controller is used.

1. *Optical Power Equalization:* First the optical power at the output of the OBFN is measured with only one input connected. After that, the optical power is checked with only the other input connected. The combiner is tuned until both inputs connected separately have the same optical power.

2. *RF Power Equalization:* After the optical power is equalized, the same procedure applies to the RF power. The RF output power of the modulators is checked. The optical output is connected to the detector, the Emcore R2860E. Which, in turn, is connected to the Spectrum Analyzer to check the RF power. At this point, we equalize the RF output power of both modulators by tuning the combiner between branches 1 and 2 of the OBFN. If the modulators have been properly set, the RF power should be already equalized.

6.2 RF Tone

The feedback loop is first tested using a single tone as RF input. As explained in Section 2.1, the project is used to receive DVB signals, which center frequency is 1.545 GHz and bandwith is 1.2 GHz. Consequently, the frequency of the tone is set at 1.545 GHz.
To generate the tone, a network analyzer is used, the Agilent PNA-L N5320A. The settings used at Port 1 in the network analyzer are:

- Sweep type = CW Time
- CW Frequency = 1.545 GHz
- Channel Power = 0 dBm

The RF signal used can be seen with the spectrum analyzer as in Figure 6.2.

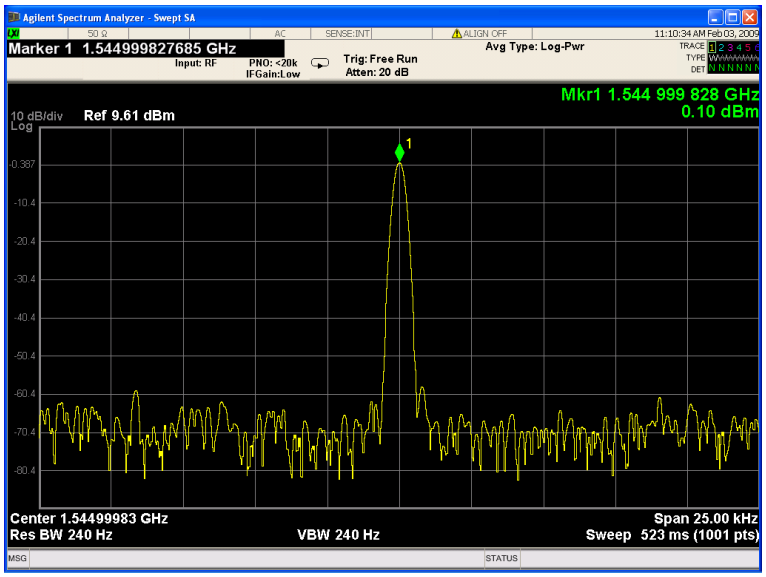

Figure 6.2: RF Tone. Center frequency = 1.545 GHz. Channel Power = 0 dBm

Discussion

Since the feedback loop designed in Section 4.3 uses different electronic devices, after setting the phase shifter and before measuring the output power, a waiting time is needed. After sending the command to set the phase shifter, the algorithm has to wait a certain time in order to assure that the desired phase shifter value is set and stable, so that the measurement of the output power with the spectrum analyzer is correct and not affected by transients.
After testing the algorithm with different waiting times, the minimum results to have

proper behaviours is 250 ms. In order to assure the correct power measurement, the delay time chosen is the double of the minimum waiting time, 500 ms. Using this value, it can be seen very clearly on the screen of the spectrum analyzer that the measurement is correct. Moreover,this time is fast enough to synchronize the optical phase when the output power is fading.

In the following measurements graphs, the X axis indicates the time samples. The graphs represent the result when the algorithm runs over a time of five minutes. The number of samples is different among the different graphs because of the different times steps (waiting times) used.

6.2.1 Hill Climbing Algorithm

As explained in Section 5.1, some parameters must be set for the HCA. The aim of the test with the tone, described in this Subsection, is to find the best values for these parameters in order to use them in the final algorithm.

Threshold Power

A threshold power is set in order to change the step used to move the phase shifter. When the output power is under the threshold, the step is bigger to increase the speed of convergence. The threshold power is set based on the maximum power at the output of the OBFN. That means that the maximum power provided by the system has to be known.
After several tests with different values, the best threshold appears to be 2 dB below the maximum power.

Fine Step

When the output power is higher than the threshold power, the phase shifter is moving more slowly. In order to select the best fine step, the HCA has been tested with different values. Figure 6.3 represents how the trend of the output power of the OBFN changes with different choices for the fine step. The step is expressed in tenths (1/10) of mV.

As can be seen, setting the fine course to 50 provides the best results. This fine step reaches the maximum power, and after that, provides the best stabilization of the ouput power. The other choices for the step, on the contrary, are not fast enough to follow the power drift.

Course Step

When the ouput power is lower than the threshold power, the phase shifter is moving faster to reach the maximum as soon as possible. In order to select the best course

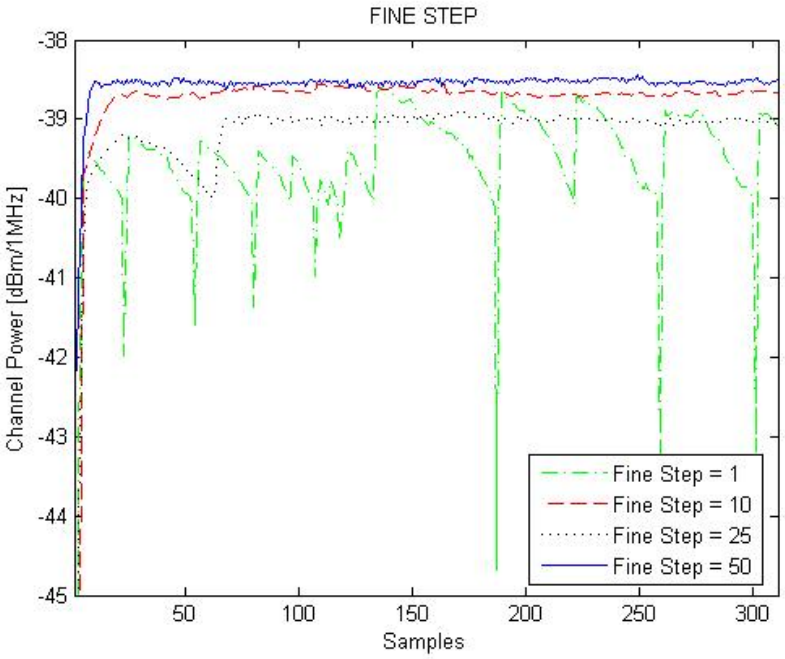

Figure 6.3: RF Tone and Hill Climbing Algorithm. Comparison of different fine steps

step, the HCA has been tested with different values. Figure 6.4 represents how the output power of the OBFN changes with different course steps.

As can be seen, the maximum ouput power is reached faster with the course step set to 500, but this is not the best course step, as explained now.
Before the threshold is reached, the course step is used: the bigger the step, the faster the maximum power is reached. Once the threshold is reached, the fine step is used. The problem appears when the ouput power decreases due to desynchronization. If the output power fades slowly and goes below the threshold, the course step is set again. Now, depending on the direction to move the phase shifter, the power can recover or can decrease, with a speed that is proportional to the value chosen for the course step. The use of a very big step is then risky, since this can lead to very low transient power before re-synchronization. If, after reaching the maximum, in the practical DVB applicattion the power decreases as in Figure 6.4, the signal would be lost, and this is unacceptable.
For this reason, the best course step is 150. The best compromise between speed to reach the maximum and efficiency after desynchronization events.

Hill Climbing Algorithm Limitations

As explained in Section 5.1.3, the hill climbing algorithm has some limitations. In theory, these limitations do not affect our system due to the implemented setup. When only two branches are used, the output power does not have a local maximum, a ridge

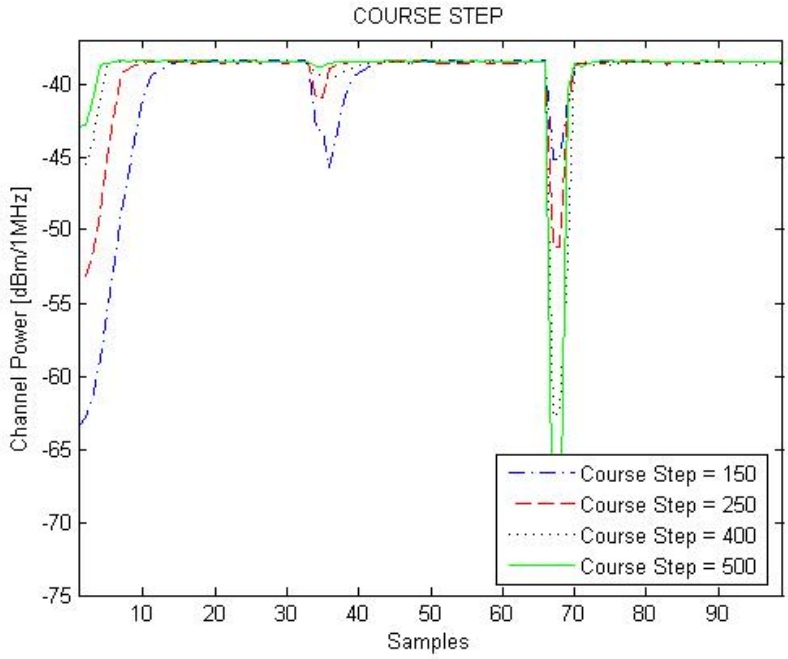

Figure 6.4: RF Tone with Hill Climbing Algorithm. Comparison of different course steps

or a plateau. On the contrary, during the test of the algorithm with the real setup, it can happen that the algorithm does not reach the maximum, and gets stuck at some point. An occurence of this problem can be seen the zoom image in Figure 6.5. The probability of this depends on the random initialization value of the phase shifter. The ripple indicates that the algorithm is stuck to a local maximum.

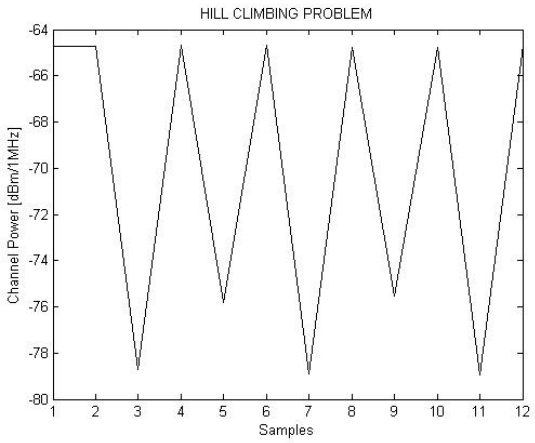

Figure 6.5: RF Tone. Hill Climbing Problem

6.2.2 Feedback Loop Algorithm

After tuning the HCA, the feedback loop algorithm implemented in Section 5.3 is tested. The HCA is set based on the results of the previous optimization:

- Threshold Power = -40 dBm
- Fine Step = 50
- Course Step = 150

The parameters of the GA are set as follows:

- Number of Iterations = 10
- Number of Individuals = 10
- Number of Bits = 12
- Mutation Probability = 0.01

The results are shown in Figure 6.6. First the Genetic Algorithm (GA) is running. After this, the maximum output power is reached and the Hill Climbing Algorithm (HCA) runs to keep the value. The vertical line in the graph separates the periods in which each algorithm is executing.

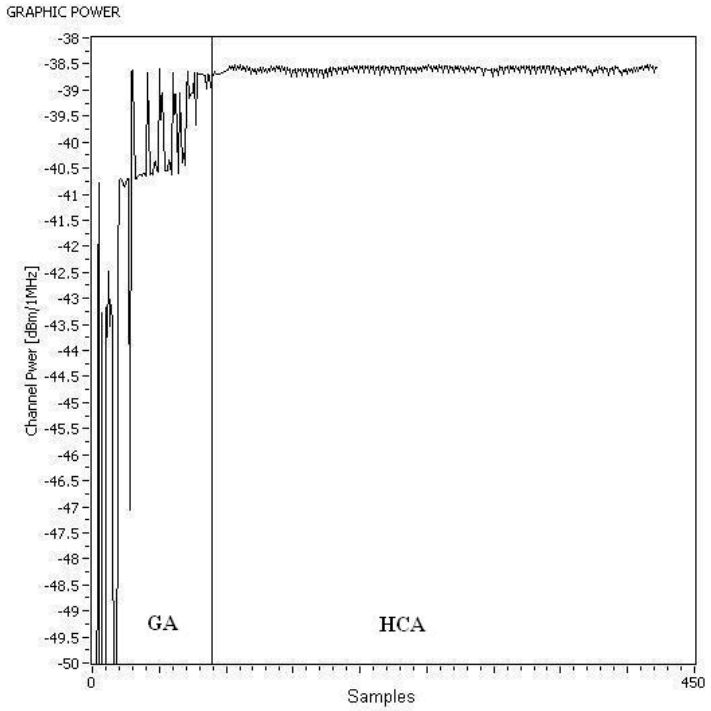

Figure 6.6: RF Tone. Feedback Loop Algorithm

As expected, after executing the GA, the global maximum power is reached. After that, the HCA is executing and stabilizing the ouput power at the maximum.

6.3 DVB Signal

After the results with a known RF tone, the feedback loop is tested with a DVB signal at the RF input in Figure 6.1. This signal is provided by a TV-SAT dish with Low-Noise Block (LNB). The scheme of the setup to obtain a DVB signal is presented in Figure 6.7.

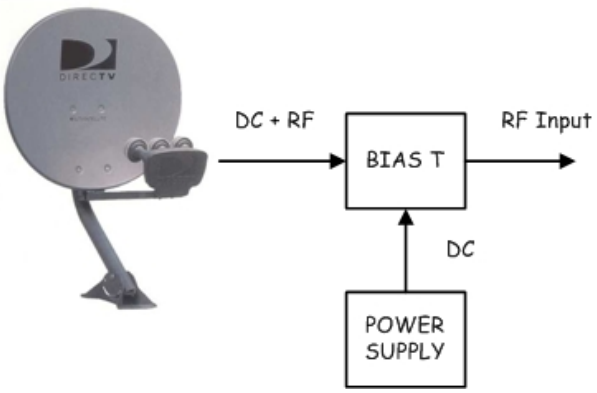

Figure 6.7: Dish Setup

The RF signal received by the dish is down converted to IF by means of a LNB. As explained in Section 2.1, the RF wave has two polarizations, which can be toggled by feeding the LNB with different voltages:

- Horizontal Polarization: DC = 19 V
- Vertical Polarization: DC = 14 V

By means of a a power supply set to 19 V and a bias T, the horizontal polarization is set and received. With this setup, the dc only feeds the LNB and after the bias T there is only RF signal.

The dish is aligned to the satellite Astra 19.2E. The signal after the bias T is connected to the spectrum analyzer to see the transponders from the satellite. Based on this, the dish is moved till the alignment is perfect and the transponders have the maximum power and can be seen clearly. The DVB signal obtained is shown in Figures 6.8 and 6.9. As can be seen, the frequency of the center transponder is 1.545 GHz, and its bandwidth is 36 MHz. The algorithm in the feedback loop uses the power of this transponder to synchronize the optical phase.

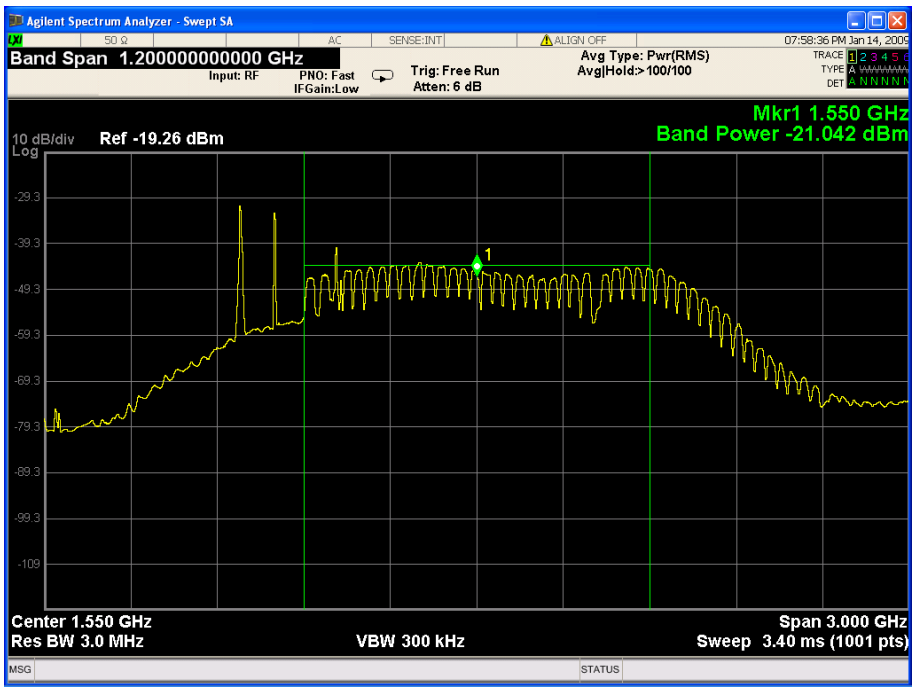

Figure 6.8: DVB Signal Transponders

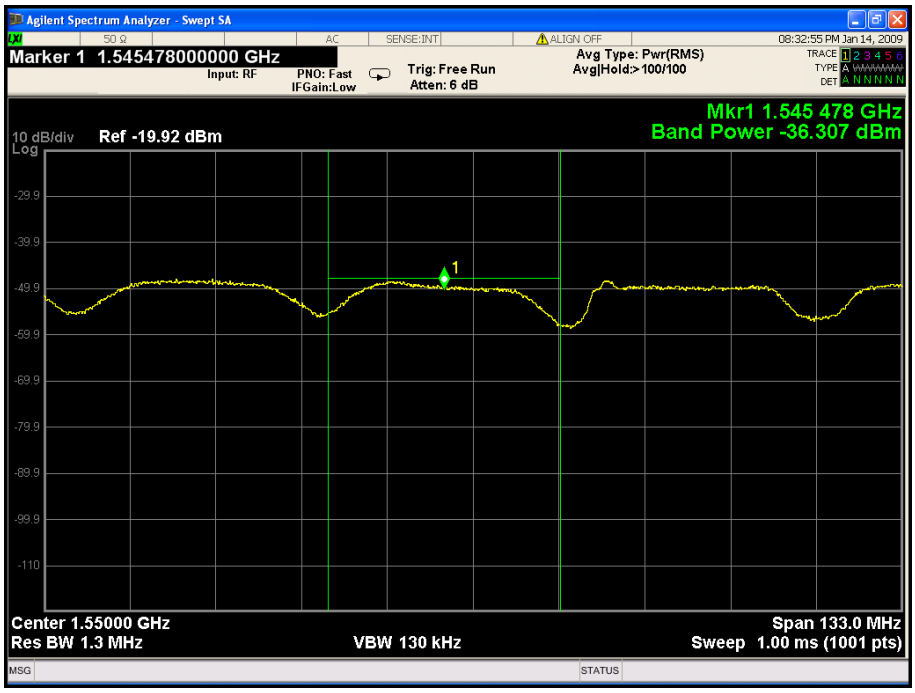

Figure 6.9: DVB Signal Center Transponder

This signal can not be connected directly to the modulators. The RF input of the OBFN should be around 0 dBm, and the DVB signal after the bias T is around -45 dBm. Due to the losses through the OBFN, if the DVB signal is connected without amplification, at the output of the OBFN there is no signal. For this reason, two LNAs are used to amplify the DVB signal after the bias T. The amplifier used is the Mini-Circuits ZRL-2400LN+. The gain of the cascade amplifier at this bandwidth is +43 dB. The final scheme to set the dish is shown in Figure 6.10.

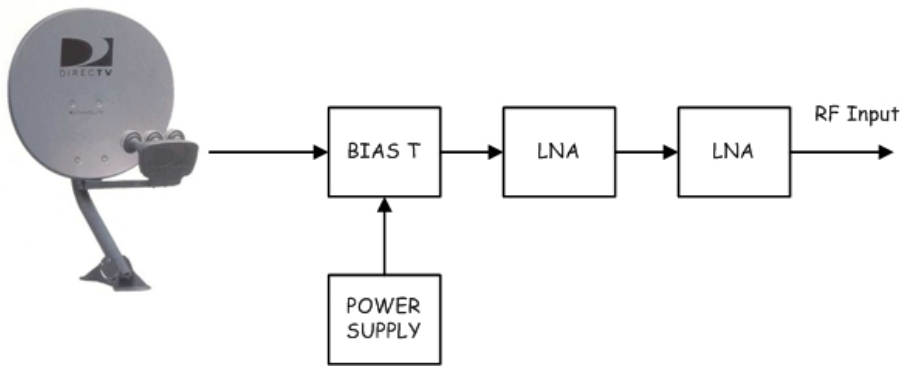

Figure 6.10: Final Dish Setup

After the dish is set, the feedback loop is tested using the DVB signal. As said before, the transponder measured is the one in the center of the bandwidth.

6.3.1 Hill Climbing Algorithm

First the HCA is tested for the DVB signal. The parameters are optimized as explained in the previoud Section. The only change in this case is the threshold power, that is set to -45 dBm. In Figure 6.11 can be seen two executions of the HCA. In this graph, the problem with the HCA is seen clearly. Depending on the initialization, the algorithm can reach either the global or a local maximum, as expected.

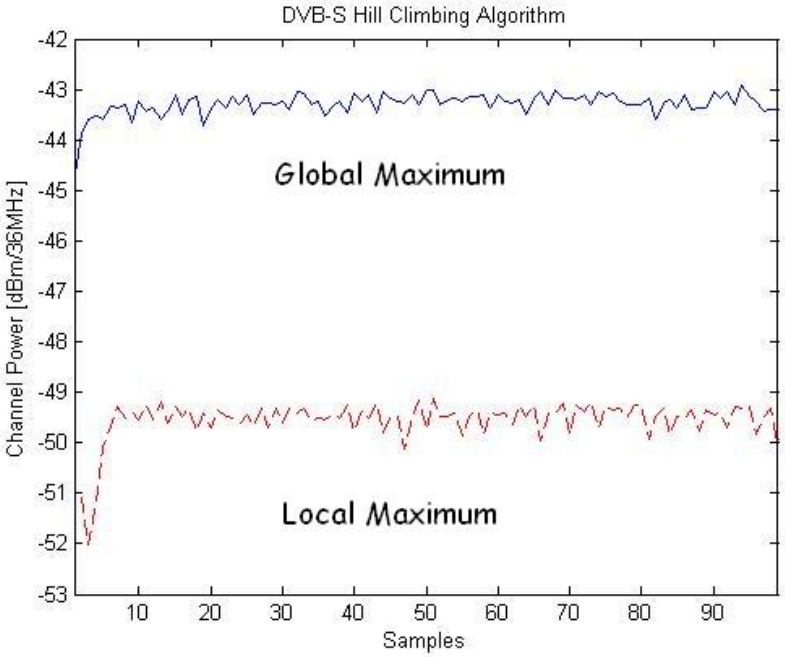

Figure 6.11: DVB Hill Climbing

6.3.2 Feedback Loop Algorithm

Finally the feedback loop algorithm is tested for the DVB signal. The parameters of the GA are set to the same values as in Subsection 6.2.2
When the algorithm is not running, the desynchronization of the optical phase appears. This can be seen in Figure 6.12 where, after the OBFN, the transponders of the DVB signal can not be distinguised.

Once the algorithm is executing, the optical phase is synchronized and the maximum ouput power is reached. As shown in Figure 6.13, now the transponders are already visible.

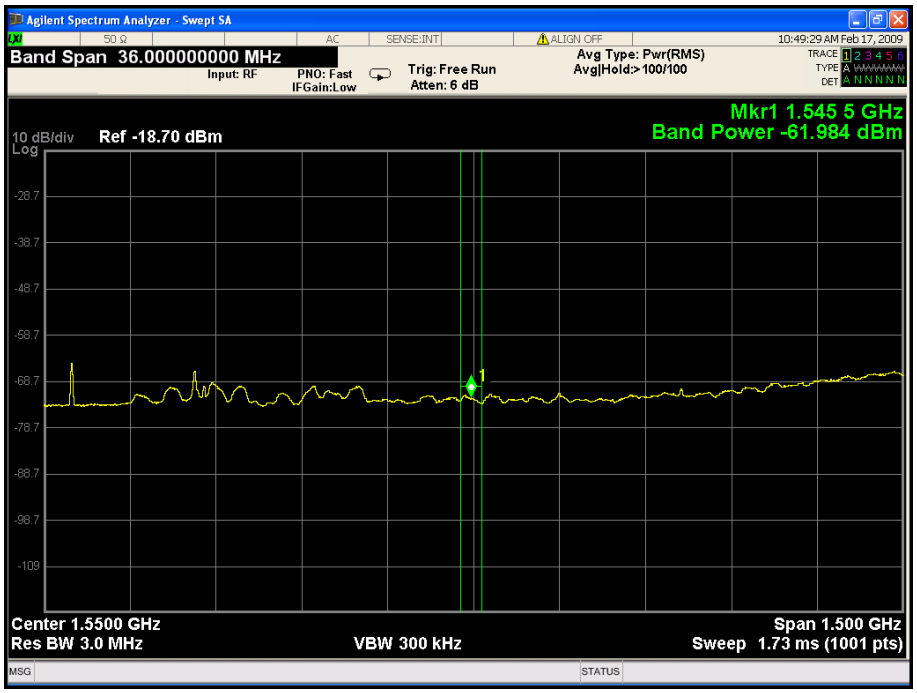

Figure 6.12: DVB Signal with OBFN Desynchronized

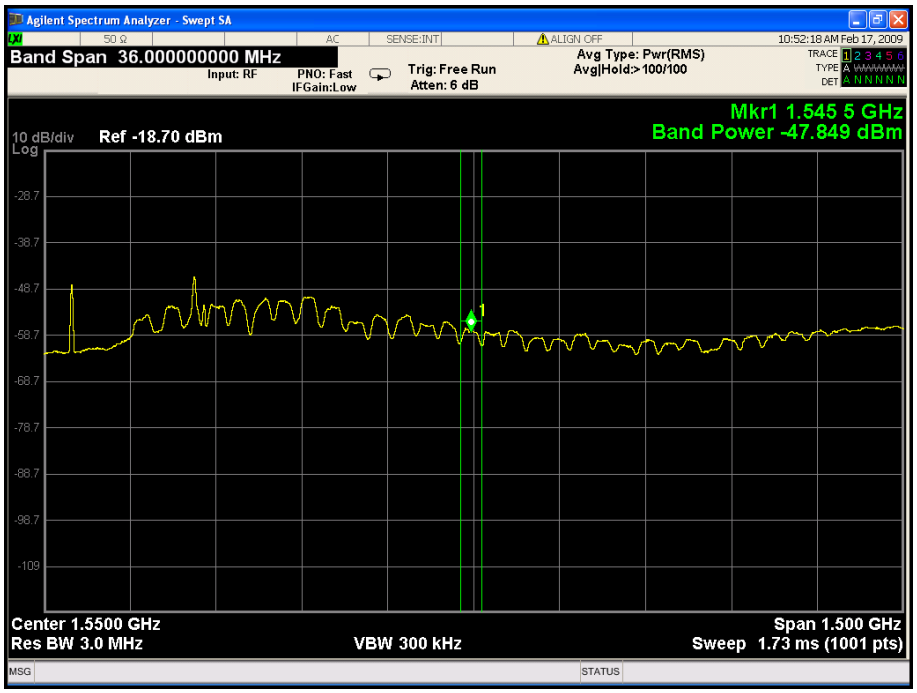

Figure 6.13: DVB Signal with OBFN Synchronized: The transponders are all clearly visible

The execution of the algorithm is shown in Figure 6.14. First, the Genetic Algorithm (GA) is running. After this, the global maximum is reached and the Hill Climbing Algorithm (HCA) runs. The vertical line in the graph indicates the switching point between the two algorithm's executions.

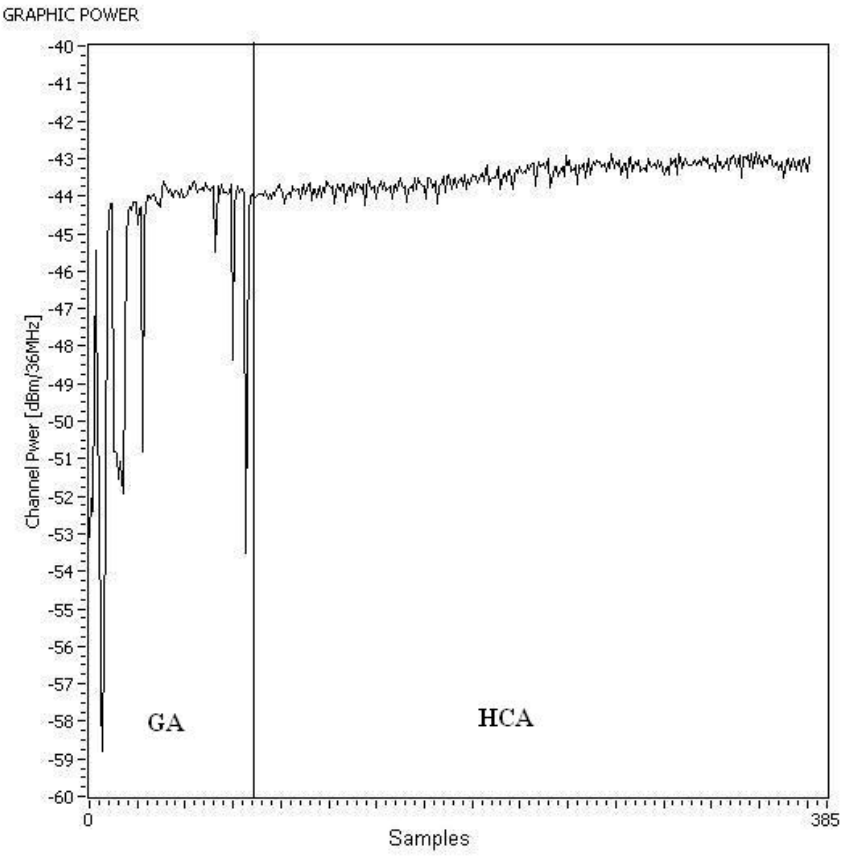

Figure 6.14: RF Tone. Feedback Loop Algorithm

6.4 Conclusions

The signal power techique is shown to be a valid solution to synchronize the optical phase. It has been proved that by means of a feedback loop, the output power is stabilized at the maximum value. The algorithm implemented for the feedback loop is successfully working in a 2x1 OBFN with one phase shifter.

Two different RF input signals have been tested: a RF tone and the wideband DVB signal from Astra satellite. The final results are successfull for both type of signals.

The different algorithms studied in Chapter 5 were tested. First, the parameters of the HCA have been optimized. After that, the limitations of the HCA have been demonstrated. To conclude the feedback loop algorithm has been tested on the real setup using the best parameters obtained before.

In order to make good measurements, the optimum parameters of the algorithm may change in another setup, depending on the noise levels and of the speed of the heater controller and the measuring devices used. For this reason, it is recommended to adjust the parameters until the best output is given.

Chapter 7

Conclusions and Recommendations

7.1 Conclusions

A feedback loop has been implemented to synchronize the optical phase in coherent optical beamformers for phased array antennas. Optical phase synchronization is extremely important for the project due to the receiver architecture used. Two different solutions for the problem have been presented and discussed: finally the signal power technique has been chosen.

The feedback loop used for this technique has been designed in Chapter 4. The loop has to be fast enough to optimise the value of the phase shifters when the output power is fading. After the research, the design that accomplish all the requirements was to use a spectrum analyzer to measure the ouput power and a computer to communicate with the heater controller.

The algorithm running continuosly in the feedback loop was simulated and tested. Based on the results, the optical phase synchronization in a 2x1 OBFN has been achieved.The experimental results showed that the parameters for different algorithms had to be set carefully in order to make the algorithm work properly.
A local search algorithm, the Hill Climbing Algorithm (HCA), and a global search algorithm, the Genetic Algorithm (GA), were studied. Both algorithms are not an optimum solution separatly. The HCA can track the power when it is fading but, depending on the initialization, it can get stuck in a local maximum. On the other side, once the GA has finished its execution it reaches the maximum but does not move the phase shifters anymore and then, when the power is fading due to desynchronization, the GA does not track the power and can not be run again because starts from the initialization. The solution implemented and tested for the feedback loop was to combine both algorithms. First the GA and later the HCA.

The conclusion is that using a feedback loop based on the power at the output of the OBFN solves the problem. As shown in the results, the solution synchronizes the optical phase in a 2x1 OBFN.

7.2 Recommendations

The first step to synchronize the optical phase in the OBFN has been accomplished, but the research has to continue.

- Firstly the algorithm has to be tested in different scenarios. The first scenario will be to simulate the reception of a wave from one direction, not only a front wave. After that, the system has to be extended to a 4x1 and, later on, to a 8x1. For the best behavior of the algorithm, the parameters have to be chosen precisely.

- The research on the algorithm is very important. Some other algorithms can be studied. Also the algorithm implement can be improved. For instance, in the GA instead of executing all the iterations until the algorithm finishes, one parameter to stop the algorithm can be added. The same reasoning as for the threshold power in the HCA can be used. When the GA has reached the threshold power, the algorithm stops. The GA does not have to wait until all the iterations finish.

- The final step for the future work will be to design a PCB board in which the scheme of the feedback loop is implemented. This board will replace the spectrum analyzer and the computer, but it is communicating with the heater controller. In an advance work, the PCB will be integrated inside the heater controller.
  This will allow a faster algorithm convergence, due to the much lower time overhead on the power measurement.

Bibliography

[1] "Telecommunication engineering group." [Online]. Available: http://www.el.utwente.nl/te/index.htm

[2] "Pidea+ project smart." [Online]. Available: http://pideaplus-smart.org/

[3] "Euripides." [Online]. Available: http://www.euripides-eureka.eu/

[4] "Lionix bv." [Online]. Available: http://www.lionixbv.nl/

[5] H. Schippers, J. Verpoorte, P. Jorna, A. Hulzinga, A. Meijerink, C. Roeloffzen, R.G.Heideman, A. Leinse, and M. Wintels, "Broadband conformal phased array with optical beam forming for airbone satellite communication," Aerospace Conference, 2008 IEEE, pp. 1–17, March 2008.

[6] C. Balanis, *Antenna Theory: Analysis and Design*. Wiley-Interscience, 2005.

[7] A. Meijerink, L. Zhuang, C. G. H. Roeloffzen, D. A. I. Marpaung, R. G. Heideman, A. Borreman, and W. van Etten, "Novel phased array receive antenna control system employing a fully integrated ring resonator-based optical beam forming network," 2007, unpublished.

[8] L. Zhuang, "Time-delay properties of optical ring resonators," Master's thesis, University of Twente. Department of Electrical Engineering. Chair of Telecommunication Engineering, May 2005.

[9] A. Meijerink, C. G. H. Roeloffzen, L. Zhuang, D. A. I. Marpaung, and W. van Etten, "Signal processing in smart satellite receivers using optical bean forming (obf)," internal report, University of Twente, June 2006.

[10] A. Nirmalathas, G. Smith, and D. Novak, "Sensitivity analysis of optical ssb generation using a dual-electrode mach-zender modulator," Microwave Photonics, 1998. MWP '98. International Topical Meeting on, October 1998.

[11] B. den Uyl, "Single sideband modulation for optical bean forming in phased array antennas," Master's thesis, University of Twente. Department of Electrical Engineering. Chair of Telecommunication Engineering, August 2006.

[12] J. P. Hevilla, "Optical sideband filtering," Master's thesis, University of Twente. Department of Electrical Engineering. Chair of Telecommunication Engineering, April 2007.

[13] L. Zhuang, C. G. H. Roeloffzen, R. G. Heideman, A. Borreman, A. Meijerink, and W. van Etten, "Single-chip optical beam forming network in lpcvd waveguide technology based on optical ring resonators," Proc. of the International Topical Meeting on Microwave Photonics (MWP'2006), Grenoble, France, 3-6 Oct. 2006, paper F1.4.

[14] ——, "Ring resonator-based single-chip 1x8 optical beam forming network in lpcvd waveguide technology," Proc. 11th IEEE/LEOS Symp., Benelux, Eindhoven, The Netherlands, pp. 45–48, 30 Nov.-1 Dec. 2006.

[15] ——, "Single-chip ring resonator-based single-chip 1x8 optical beam forming network in cmos-compatible waveguide technology," IEEE Photon. Technol. Lett., Grenoble, France, pp. 1130–1132, August 200.

[16] J.-W. van 't Klooster, "Context, design and implementation of a control system for ring resonator-based optical beam forming networks," Master's thesis, University of Twente. Department of Electrical Engineering. Chair of Telecommunication Engineering, October 2008.

[17] M. Ruiter, "Design of a system for driving heaters on optical ring resonators," Master's thesis, University of Twente. Department of Electrical Engineering. Chair of Telecommunication Engineering, 2006.

[18] T. Vrijmoeth, "Implementation of a heater-driving system," Master's thesis, University of Twente. Department of Electrical Engineering. Chair of Telecommunication Engineering, 2007.

[19] T. Jansen, "Implementing a heater controller for optical beam forming networks," Master's thesis, University of Twente. Department of Electrical Engineering. Chair of Telecommunication Engineering, 2007.

[20] "National instruments labview." [Online]. Available: http://www.ni.com/labview/

[21] R. Griffin, D. Sampson, and D. Jackson, "Demonstration of data transmission using coherent correlation toreconstruct a coded pulse sequence," *Photonics Technology Letters, IEEE*, vol. 4, no. 5, pp. 513–515, 1992.

[22] A. Meijerink, C. G. H. Roeloffzen, R. Meijerink, L. Zhuang, D. A. I. Marpaung, M. bentum, J. Verpoorte, A. Hulzinga, and W. van Etten, "Novel ring resonator-based integrated photonic beamformer for broadband phased array receive antennas – part i: Design and performance analysis," internal report, University of Twente, unplublished.

[23] M. Mitchell, *An Introduction to Genetic Algorithms*. Bradford Books, 1996.

Appendix A

Hill Climbing Algorithm Code

This Appendix shows the code of the Hill Climbing algorithm in Matlab. The operation of this algorithm is explained in Chapter 5.

```
% The range of the phase shifters are from 0 to 3000.
% We have set the direction to change the phase shifters like:
% Direction = 0 <-- LEFT
% Direction = 1 --> RIGH

% Firstly we set the new phase shifter to the previous value, so in
% case we have not change it, the next phase shifter will be the same.
next_phase_shifter = phase_shifter;

% If the power is less than a threshold power desired, we change the
% step for a bigger one: Course step
if power < threshold
  step = course_step;
end

% If the power with the new phase shifter is more than the power with
% the previous one
if power > power_before
  %Check the direction we are moving the phase shifter
  if direction == 1
  % If we are moving right, we continue moving in tihs direction
  % (add the step)
    next_phase_shifter = phase_shifter + step;
  else
  % If we are moving left, we continue moving in tihs direction
  % (subtract the step)
```

```
    next_phase_shifter = phase_shifter - step;
  end
end

% If the power with the new phase shifter is less than the power with
% the previous one came back to the previous value and change the
% direction to the opposite.
if power < power_before
  if direction == 1
    direction = 0;
    next_phase_shifter = phase_shifter - step;
  else
    direction = 1;
    next_phase_shifter = phase_shifter + step;
  end
end

% If the new phase shifter value is less than 0 (negative), then the
% new value will be 0 and the direction change from 0 to 1.
if next_phase_shifter < 0
  next_phase_shifter = 3000;
end

% If the new phase shifter value is more than 3000, then the new value
% will be 0 and the direction change from 0 to 1.
if next_phase_shifter > 3000
  next_phase_shifter = 0;
end

% Finally the power before is updated.
power_before_output = power;
```

Appendix B

Genetic Algorithm Code

This Appendix shows the code of the Genetic algorithm in Matlab. The operation of this algorithm is explained in Chapter 5.

```
% First the individuals are coded in binary
aux_individuals = individuals;
aux_binary_individuals = dec2bin(aux_individuals,12);

% Because of dec2bin Matlab function, the matrix has to
% be reordered
for i = 1:Number_individuals
k = i;
l=1;
   for j = 1:(Number_Phase_Shifters*12)
      if l == 13
         k = k + number_individuals;;
         l = 1;
      end
      binary_individuals(i,j) = aux_binary_individuals(k,l);
      l = l + 1;
   end
end

% The best individual's position in the matrix is found
[best_power_measurement index] = max(fitness);
best_individual = [aux_individuals(index,:)];

% Crossing Reproduction

crossing_point = round(rand*(12-2))+1;
```

```
fitness_aux = fitness;
better_half_indexes = [];

for i=1:round(number_individuals)/2
   [maximum index_aux] = max(fitness_aux);
   fitness_aux(index_aux) = -1000;
   better_half_indexes = [better_half_indexes index_aux];
end

individuals_after_crossing_b = binary_individuals;

for i = 1:length(better_half_indexes)

   subject1 = binary_individuals(better_half_indexes(i),:);
   chosen = i;

   while (chosen == i)
      chosen = 1 + round((length(better_half_indexes)-1)*rand);
   end

  subject2 = binary_individuals(better_half_indexes(chosen),:);

   individuals_after_crossing_b(2*i-1,:) = [subject1(1:crossing_point)
subject2(crossing_point+1:num_bits)];
   individuals_after_crossing_b(2*i,:) = [subject2(1:crossing_point)
subject1(crossing_point+1:num_bits)];
end

% Mutation
new_generation_b = individuals_after_crossing_b;

for i = 1:number_individuals
   for j = 1:num_bits
      if rand < prob_mut
         if (individuals_after_crossing_b(i,j) == '0')
            new_generation_b(i,j) = '1';
         else
            new_generation_b(i,j) = '0';
         end
```

```
      end
   end
end

% As done before, the matrix has to be reordered before converting
% from binary to decimal

k =1;
l=1;
for i = 1:Number_Phase_Shifters*number_individuals
   for j = 1:12
      if l == (12*Number_Phase_Shifters+1)
         k = k +1;
         l = 1;
      end
      aux_new_generation_b(i,j) = new_generation_b(k,l);
      l = l + 1;
   end
end

aux_new_individuals = bin2dec(aux_new_generation);

% After converting to decimal the higher value has to be 3000
for i=1:length(aux_new_individuals)
   if aux_new_individuals(i) > 3000
      aux_new_individuals(i) = 3000;
   end
end

% After converting to decimal, the matrix has to be reordered again
% to mantain the same format
k =1;
for i = 1:number_individuals
   for j = 1:Number_Phase_Shifters
      new_individuals_b(i,j) = aux_new_individuals(k);
      k = k + 1;
   end
end
```

Index